# Reactivity Patterns of Carbyne Hydride Complexes of Tungsten

Ewald Bannwart, Heiko Jacobsen, Franck Furno, and Heinz Berke*

*Anorganisch-chemisches Institut der Universität Zürich, Winterthurerstrasse 190, CH-8057 Zürich, Switzerland*

*Received February 11, 2000*

Tungsten carbyne chlorides of the type W(CMes)(CO)(Cl)$L_2L'$ (L = $P(OMe)_3$, L′ = CO (**2a**); L = $PMe_3$, L′ = CO (**2b**); L = $P(O^iPr)_3$, L′ = pyridine (py) (**2c**); L = $PPh_3$, L′ = CO (**2d**); 2L = $Ph_2PCH_2CH_2PPh_2$, L′ = CO (**2e**)), W(CMes)(CO)(Cl)$L_3$ (L = $P(OMe)_3$ (**3a**); L = $PMe_3$ (**3b**); 3L = $Ph_2PCH_2CH_2)_2PPh$ (**3d**)), and W(CMes)(Cl)$L_4$ (L = $P(OMe)_3$ (**4a**)) have been prepared by starting from W(CMes)$(CO)_2$(Cl)$(py)_2$ (**1**). Treatment of the chloride complexes with $NaBH_4$ in THF furnished the borohydride adducts W($\eta^2$-$H_2BH_2$)(CMes)(CO)$L_2$ (L = $P(OMe)_3$ (**5a**); L = $PMe_3$ (**5b**); L = $P(O^iPr)_3$ (**5c**); L = $PPh_3$ (**5d**)) and W($\eta^2$-$H_2BH_2$)(CMes)$L_3$ (L = $P(OMe)_3$ (**6a**)), which served as precursors for new tungsten carbyne hydrides. The compounds W(CMes)(CO)(H)$L_3$ (L = $P(OMe)_3$ (**7a**); L = $PMe_3$ (**7b**); 3L = $(Ph_2PCH_2CH_2)_2PPh$ (**7d**)) and W(CMes)(H)$L_4$ (L = $P(OMe)_3$ (**8a**)) were obtained from the reaction of the borate complexes **5a**,**b**,**d** and **6a** with quinuclidine in THF at −20 °C in the presence of excess phosphorus donor ligands. The hydrides can be kept and characterized at low temperatures but decompose when warmed to room temperature. The reactivity of this novel class of compounds has been investigated for **7a**, which reacts even at low temperatures with phenol, carbon dioxide, and unsaturated organic compounds. In the presence of excess phosphorus donor ligands or CO, **7a** rearranges into the carbene complexes W(CHMes)(CO)(L)(L′)$(P(OMe)_3)_2$ (L = L′ = $P(OMe)_3$ (**15a**); L = L′ = $PMe_3$ (**15b**); L = $P(OMe)_3$, L′ = CO (**16**)) via intramolecular hydride migration. A similar reaction could not be observed for **7d** or **8a**. Density functional calculations support the notion that this transformation is initiated by ligand dissociation and that formyl species are not likely to occur as reaction intermediates. Reaction of **3a** with HCl provides access to another carbene complex, W(CHMes)$(Cl)_2(CO)(P(OMe)_3)_2$ (**17**). It was concluded from NMR spectroscopy that the carbene ligand in the $d^4$ complex **17** pivots in place to establish an $\eta^2$-type coordination with an agostic interaction.



## Introduction

In recent years our group has studied the chemistry of activated transition-metal hydrides. In this context, systematic investigations were carried out on how ancillary ligands might activate the transition-metal−hydrogen bond. It could be shown that the nitrosyl ligand plays an outstanding role in the electronic activation of hydride units,[1] especially those disposed *trans* to NO. Among other effects, the NO group displays a strong *trans* influence, causing a concomitant weakening of the metal−ligand bond. Although the H ligand too behaves as a *trans* influence moiety, the multiply bonded NO group always prevails in the electronic competition for $\sigma$-type d-orbital overlap. Thus, $H^{t-NO}$ ligands are less strongly bound and display an overall high reactivity with a great potential for insertion reactions.[2,3] As further consequence of the aforementioned reduced $L_nM-H$ overlap, one would also expect additional enhancement of the a priori hydridic polarization of the $L_nM-H$ bond. Qualitative MO considerations provide a clear explanation for this effect. The interaction diagram for the formation of the M−H bond is presented in Chart 1. As a result of second-order

**Chart 1**

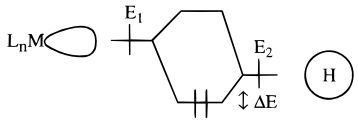


perturbation theory,[4] the energetic stabilization $\Delta E$ is proportional to the square of the overlap $S^2$ between the interacting fragment orbitals but inverse proportional to the absolute difference of their unperturbed energies. Diminishing $S$ leads to a smaller value for $\Delta E$, which in turn increases the H contribution to the $L_nM-H$ bonding orbital and consequently leads to an enhanced hydricity.

(1) Berke, H.; Burger, P. *Comments Inorg. Chem.* **1994**, *16*, 279.
(2) (a) Kundel, P.; Berke, H. *J. Organomet. Chem.* **1987**, *335*, 353. (b) van der Zeijden, A. A. H.; Sontag, C.; Bosch, H. W.; Shklover, V.; Berke, H.; Nanz, D.; von Philipsborn, W. *Helv. Chim. Acta* **1991**, *74*, 1194. (c) van der Zeijden, A. A. H.; Bosch, H. W.; Berke, H. *Organometallics* **1992**, *11*, 2051. (d) van der Zeijden, A. A. H.; Berke, H. *Helv. Chim. Acta* **1992**, *75*, 513. (e) Nietlispach, D.; Bosch, H. W.; Berke, H. *Chem. Ber.* **1994**, *127*, 2403.
(3) (a) Bäth, F. Ph.D. Thesis, Universität Zürich, 1998. (b) Höck, J.; Fox, T.; Schmalle, H.; Berke, H. *Chimia* **1999**, *53*, 350. (c) Liang, F.; Jacobsen, H.; Schmalle, H.; Artus, G.; Berke, H. *Organometallics*, in press.
(4) Albright, T. A.; Burdett, J. K.; Whangboo, M.-H. *Orbital Interaction in Chemistry*; Wiley: New York, 1985; Chapter 3.

10.1021/om000129h CCC: $19.00 
Publication on Web 08/03/2000

To further explore the possibilities of tuning the metal hydrogen bond, we replaced the activating NO group with a carbyne CR. This ligand is also known to display a strong *trans* influence.[5] It is classified as a three-electron donor and, thus, acts as an isoelectronic stand-in for NO. In comparison to the nitrosyl ligand, the carbyne moiety displays altered $\pi$ bonding properties and might provide a different electronic environment for $H^{t-CR}$. Therefore, it is of interest to compare the reactivity patterns of $W(\equiv CR)(CO)_nL_{4-n}H$ complexes with those of the related NO-substituted species $W(NO)(CO)_nL_{4-n}H$.

The only previously reported *trans* carbyne hydride complex with $H^{t-CR}$ is a $W(C^tBu)(dmpe)_2H$ species,[6] which was obtained from the reaction of a (neopentyl)(neopentylidene)(neopentylidyne)(dmpe)tungsten complex with dmpe (dmpe = $(Me)_2PCH_2CH_2P(Me)_2$). However, the preparation of this compound as described in the literature seems to be a very special case and is not suitable as a general standard procedure. For this reason we attempted the development of new routes to carbyne hydride tungsten species $W(\equiv CR)(CO)_nL_{4-n}H$. Our CR residue of choice is the sterically quite crowded mesitylcarbyne ligand, for which the nondesirable attack on the carbyne moiety was estimated to be less feasible.[7] For L we used a variety of phosphine ligands with different $\sigma$-donor strengths, including $P(Ph)_3$, $P(O^iPr)_3$, $P(OMe)_3$, and $PMe_3$, as well as the chelating ligands dppe (dppe = $Ph_2PCH_2CH_2PPh_2$) and $(Ph_2PCH_2CH_2)_2PPh$.

## Results and Discussion

**Synthesis of *trans*-W(CMes)(CO)$_n$(Cl)L$_{4-n}$ Complexes.** Preparative access to $W(CMes)(CO)_nClL_{4-n}$ complexes was accomplished by a Fischer type carbyne route[8] via a chloro(mesitylcarbyne)tetracarbonyltungsten intermediate, which was obtained by the reaction of the appropriate acylate complex with oxalic acid dichloride. According to the modification of Mayr,[9] an initial and unstable tetracarbonyl species was trapped by substitution of two CO groups with pyridine (py) to yield the chlorodicarbonyl(mesitylcarbyne)bis(pyridine)-tungsten system **1** (Scheme 1). Chloro(mesitylcarbyne)-tetracarbonyltungsten could, however, be traced by IR spectroscopy in methylene chloride solution.[10] Three $\tilde{\nu}$-(CO) bands are observed at 2123 (m), 2034 (s, br), and 1954 (m) $cm^{-1}$.

Compound **1** was obtained as orange crystals in almost quantitative yield. Characteristic spectroscopic

**Scheme 1**

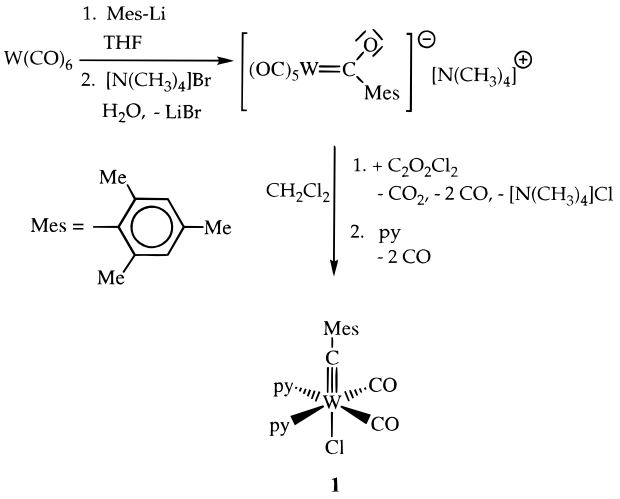


**1**

data are the two intense $\tilde{\nu}$(CO) bands at 1976 and 1889 $cm^{-1}$ (KBr) in the IR spectrum and resonances at 266.9 and 221.9 ppm for the $C_{carbyne}$ and the $C_{CO}$ atoms in the $^{13}C\{^1H\}$ NMR spectrum. It was further identified by a correct elemental analysis and its mass spectrum.

Chloro(mesitylcarbyne)tetracarbonyltungsten (**1**) served as a starting material for further ligand substitutions (Scheme 2). Its reaction with phosphorus donors produced in a first step disubstituted complexes. For $P(OMe)_3$, $PMe_3$, and the bidentate dppe, a displacement of both pyridine ligands resulted in formation of **2a**,**b**,**e**, respectively. In these complexes, the two carbonyl ligands are arranged in *cis* positions. In the case of substitution of **1** with triphenylphosphine, a similar *cis* complex could only be observed as an intermediate in the substitution reaction. IR and $^{31}P$ NMR spectroscopy indicate that in a first step a monosubstituted product is formed, which is followed by a disubstituted *cis* complex. This compound constitutes a second intermediate at low steady-state concentration, which gradually vanishes on being transformed into the thermodynamically stable *trans* compound **2d**. Also, the reaction of **1** with $P(O^iPr)_3$ resulted in the *trans* complex **2c**, presumably for steric reasons, which too are responsible for the *trans* arrangement in **2d**. The poor electron donor $P(O^iPr)_3$ does not supply enough electron density at the metal center to support an electronically unfavorable *trans* arrangement of two strong $\pi$ acceptors, so that in this case one carbonyl and one pyridine ligand are substituted for two phosphorus donors.

In the presence of an excess of the appropriate monodentate ligand or the tridentate phosphorus donor $(Ph_2PCH_2CH_2)_2PPh$, the trisubstituted species **3a**,**b**,**d** were obtained, whereby successive substitution of both pyridine ligands and one CO ligand occurred. Subsequent transformations of **3a** with $P(OMe)_3$ in neat $P(OMe)_3$ at 120 °C gave **4a** in good yield. Although it was not possible to obtain a satisfying elemental analysis, the isolated material was sufficiently pure to be used in further conversions.

The structures of the pseudo-octahedral species **2a**−**e**, **3a**,**b**,**d,** and **4a** were assigned on the basis of IR and NMR spectroscopy, as well as mass spectrometry. **2b**−**e** and **3a**,**b**,**d** were additionally confirmed by their elemental analyses. The disubstituted *cis* complexes **2a**,**b**,**e**

(5) (a) Lee, F. W.; Chan, M. C. W.; Cheung, K. K.; Che, C. M. *J. Organomet. Chem*. **1998**, *563*, 191. (b) Zhang, L.; Gamasa, M. P.; Gimeno, J.; Carbajo, R. J.; Lopez Ortis, F.; Lanfranchi, M.; Tiripicchio, A. *Organometallics* **1996**, *15*, 4274.

(6) (a) Clark, D. N.; Schrock, R. R. *J. Am. Chem. Soc.* **1978**, *100*, 6774. (b) Holmes, S. J.; Clark, D. N.; Turner, H. W.; Schrock, R. R. *J. Am. Chem. Soc.* **1982**, *104*, 6322.

(7) (a) Fischer, H.; Hofmann, P.; Kreissl, F. R.; Schrock, R. R.; Schubert, U.; Weiss, K. *Carbyne Complexes*, VCH: Weinheim, Germany, 1988. (b) Mayr, A.; Hoffmeister, H. *Adv. Organomet. Chem*. **1991**, *32*, 227.

(8) Fischer, E. O.; Maasböl, A. *Chem. Ber.* **1967**, *100*, 2445.

(9) (a) Mayr, A.; Asarao, M. F.; Kjelsberg, M. A.; Lee, K. S.; Van Engen, D. *Organometallics* **1987**, *6*, 432. (b) McDermott, G. A.; Dorries, A. M.; Mayr, A. *Organometallics* **1987**, *6*, 925. (c) Steil, P.; Mayr, A. Z. *Naturforsch., B* **1992**, *47*, 656. (d) Yu, M. P. Y.; Mayr, A.; Cheung, K.-K. *J. Chem. Soc., Dalton Trans*. **1998**, 475. (e) Yu, M. P. Y.; Cheung, K.-K.; Mayr, A. *J. Chem. Soc., Dalton Trans*. **1998**, 2723.

(10) Fischer, E. O.; Kreis, G. *Chem. Ber*. **1976**, *109*, 1673.

**Scheme 2**

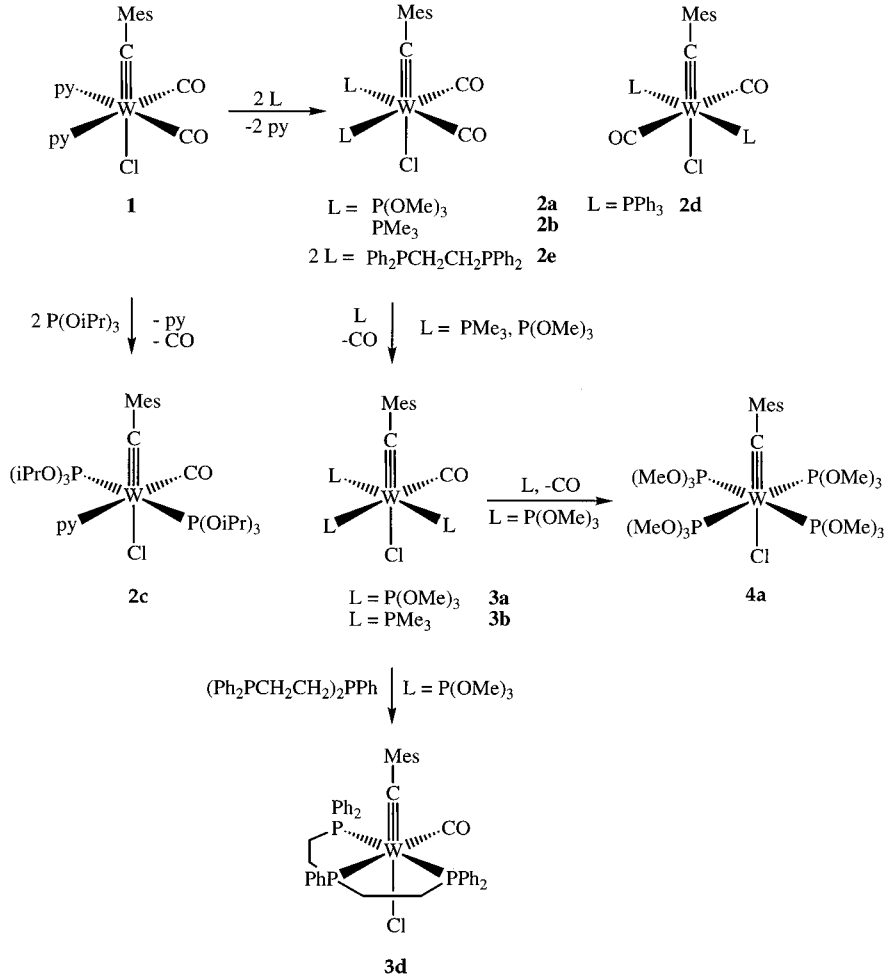


show two $\tilde{\nu}$(CO) bands in agreement with the bent arrangement of the two CO groups. The positions of these bands follow the expected order **2a** (2021, 1960) > **2e** (1997, 1913) > **2b** (1989, 1913 $cm^{-1}$), reflecting the increasing donating abilities of the phosphorus donors in this row. A less clear dependency of the $\tilde{\nu}$(CO) bands is given in the trisubstituted series of **3a** (1946) > **3b** (1891) > **3d** (1882 $cm^{-1}$), where the significant structural differences of the inner coordination sphere may play a role and account for the deviation from the purely electronic order expected from the donating properties of the phosphorus donor moieties. Compound **2c**, with two phosphorus donors and one nitrogen donor, exhibits an even lower $\tilde{\nu}$(CO) band at 1870 $cm^{-1}$. For these molecules and **4a**, further spectroscopic characteristics with some structural implications are the $^{13}C$ NMR signals of the $C_{carbyne}$ atoms, which appear between 260 and 280 ppm.

**Synthesis of W(CMes)($\eta^2$-$H_2BH_2$)$(CO)_nL_{3-n}$ Complexes.** Approaching the preparation of carbyne hydride complexes, we first aimed at the synthesis of respective borohydride compounds, since their existence and potential use as synthetic intermediates was inferred from the supposedly analogous nitrosyl hydride chemistry.[11] When complexes **2c**,**d**, **3a**,**b**, and **4a** were reacted with sodium borohydride in THF, the corresponding $\eta^2$-$BH_4$ compounds **5a**−**d** and **6a** were formed. All complexes could be isolated as red solids (**5b**,**d**) or red oils (**5a**,**c**, **6a**) in yields over 80% (Scheme 3).

**Scheme 3**

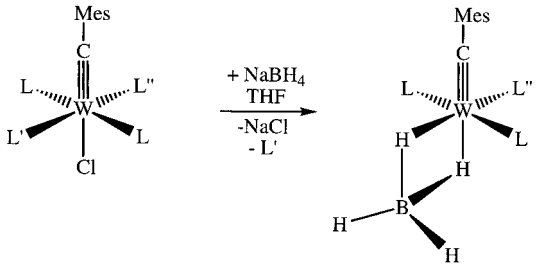


| | | | |
|---|---|---|---|
| L = L' = P(OMe)3, L" = CO | **3a** | L =P(OMe)3, L" = CO | **5a** |
| L = L' = PMe3, L" = CO | **3b** | L =PMe3, L" = CO | **5b** |
| L = P(OiPr)3, L' = py, L" = CO | **2c** | L =P(OiPr)3, L" = CO | **5c** |
| L = PPh3, L' = L" = CO | **2d** | L =PPh3, L" = CO | **5d** |
| L = L' = L" = P(OMe)3 | **4a** | L = L" = P(OMe)3 | **6a** |

The structures of **5a**−**d** and **6a** were assigned on the basis of their spectroscopic data. In the solution IR spectra (benzene or hexane), two bands at around 2400 $cm^{-1}$ ($\Delta\tilde{\nu}$ between 28 and 42 $cm^{-1}$) were attributed to $\tilde{\nu}$(BH) for the terminal hydrogens. This splitting is characteristic for a $BH_4^-$ ligand bound in bidentate fashion.[12] Stretching frequencies for the bridging hy-

(11) (a) Gusev, D. G.; Llamazares, A.; Artus, G.; Jacobsen, H.; Berke, H. *Organometallics* **1999**, *18*, 75. (b) Jacobsen, H.; Heinze, K.; Llamazares, A.; Schmalle, H. W.; Artus, G.; Berke, H. *J. Chem. Soc., Dalton Trans.* **1999**, 1717.

**Scheme 4**

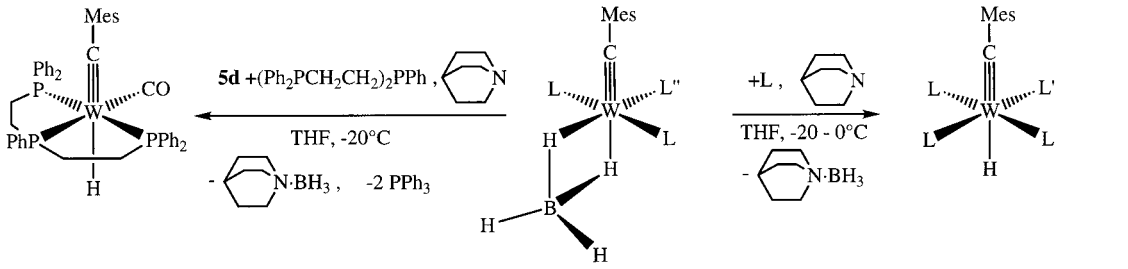


**7d**

L =P(OMe)$_3$, L' = CO **5a**
L =PMe$_3$, L' = CO **5b**
L =PPh$_3$, L' = CO **5d**
L = L' = P(OMe)$_3$ **6a**

L =P(OMe)$_3$, L' = CO **7a**
L =PMe$_3$, L' = CO **7b**
L = L' = P(OMe)$_3$ **8a**

drogen atoms,[12] which might appear in the range of 1650−2150 cm$^{-1}$, could not be assigned. For the unique CO groups of **5a**−**d,** $\tilde{\nu}$(CO) bands were identified at relatively low wavenumbers, indicating strong charge transfer from the apparently electron-rich metal center. $^{13}$C NMR resonances of the $C_{carbyne}$ atoms are shifted by about 20 ppm to lower field and are now detected between 280 and 300 ppm. For **5a**−**d**, both the bands of $C_{carbyne}$ as well as $C_{carbonyl}$ appear as triplets, which indicates that both the CR and the CO group are in *cis* positions with respect to the two phosphorus donors. In contrast to related W(CO)$_2$($\eta^2$-H$_2$BH$_2$)L$_2$(NO) molecules,[13] the carbyne complexes are relatively stable and can be stored at −20 °C, whereas the nitrosyl complexes decompose with elimination of H$_3$B·PR$_3$.[14]

**Synthesis of *trans*-W(CMes)(CO)$_n$HL$_{4-n}$ Complexes**. Two steps are necessary in order to transform the tetrahydroborate adducts into the desired carbyne hydride complexes. A Lewis base is needed in order to abstract borane, and an additional donor ligand is required to obtain a coordinatively saturated 18-electron species. The Lewis base of choice for the abstraction reaction is quinuclidine. The resulting adducts are very stable compounds, and in the presence of phosphorus donors in the reaction mixture, no H$_3$B·PR$_3$ adducts could be detected by NMR spectroscopy. Furthermore, quinuclidine as a ligand does not compete with the phosphorus donors for coordination to the metal center but selectively binds liberated BH$_3$. The role of the additional donor ligand is best taken by the corresponding phosphine.

The tetrahydroborate adducts **5a**,**b**,**d** are reacted with 1 equiv of quinuclidine and 1 equiv of PR$_3$ in THF at −20 °C to afford the tungsten carbyne hydrides **7a**,**b**,**d** (Scheme 4). For the preparation of *trans*-W(CMes)H(P(OMe)$_3$)$_4$ (**8a**), a slight excess of the amine and the phosphorus donor is required.

Complex **7a** was obtained after a reaction time of 2 h in a spectroscopic yield of 80%. No more of the starting material **5a** could be detected in the NMR spectrum. The reaction mixture might be kept for several days at −20 °C, and it is also possible to isolate the hydride at low temperatures and to store it at −20 °C. Warming to room temperature, however, leads to decomposition within 1 h. The formation of **7b** did not occur at −20 °C but required higher temperatures around 0 °C and longer reaction times. Under these conditions, the decomposition of the final product already takes place, so that the spectroscopic yield amounts only to 35%.

If the reaction of **5b** with quinuclidine and PMe$_3$ is carried out at −20 °C, the monodentate BH$_4^-$ adduct W(CMes)($\eta^1$-HBH$_3$)(CO)(PMe$_3$)$_3$ (**9b**) can be detected in the NMR spectrum. A similar species, **9a**, can also be generated from the reaction of **5a** with P(OMe)$_3$ (Scheme 5). In this case, however, it is necessary to

**Scheme 5**

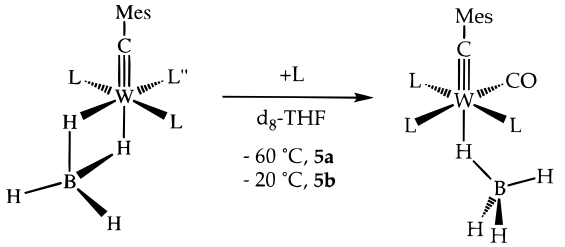


L = P(OMe)$_3$ **5a**
L = PMe$_3$ **5b**

L = P(OMe)$_3$ **9a**
L = PMe$_3$ **9b**

lower the temperature to −60 °C, since otherwise loss of BH$_3$ to form the tungsten hydride **7a** occurs, as well as back-reaction to regenerate the bidentate adduct **5a**.

This observation might give a first indication of the metal−hydride bond strength in complexes with P(OMe)$_3$ and PMe$_3$ ligands. A stronger W−H bond facilitates the B−H bond cleavage and, thus, the BH$_3$ abstraction. The higher thermal stability of **9b** compared to that of **9a** leads to the conclusion that the W−H linkage is weaker in the first case. Since the hydride ligand has also to compete with the phosphorus ligands for $\sigma$ donation to the metal center, it should bind more strongly when the donor ability of the PR$_3$ ligand is poorer, as is the case for **9a** compared to **9b.** We were also able to identify the major byproducts in the formation of **7a** and **7b**. In both cases, a complex of the type W(CO)(PR$_3$)$_5$ could be spectroscopically detected.

An alternative synthetic route to **7b** is the reaction of the PPh$_3$-substituted complex **5d** with excess trimethylphosphine and quinuclidine at low temperature. The poor donor ligand triphenylphosphine is easily exchanged with the more basic PMe$_3$ group, and instant formation of **9b** is observed. This procedure, however, did not enhance the yield of the product.

(12) Marks, T. J.; Kolb, J. R. *Chem. Rev*. **1977**, *77*, 263.
(13) van der Zeijden, A. A. H.; Shklover, V.; Berke, H. *Inorg. Chem*. **1991**, *30*, 4393.
(14) van der Zeijden, A. A. H.; Berke, H. *Helv. Chim. Acta* **1992**, *75*, 513.

**Scheme 6**

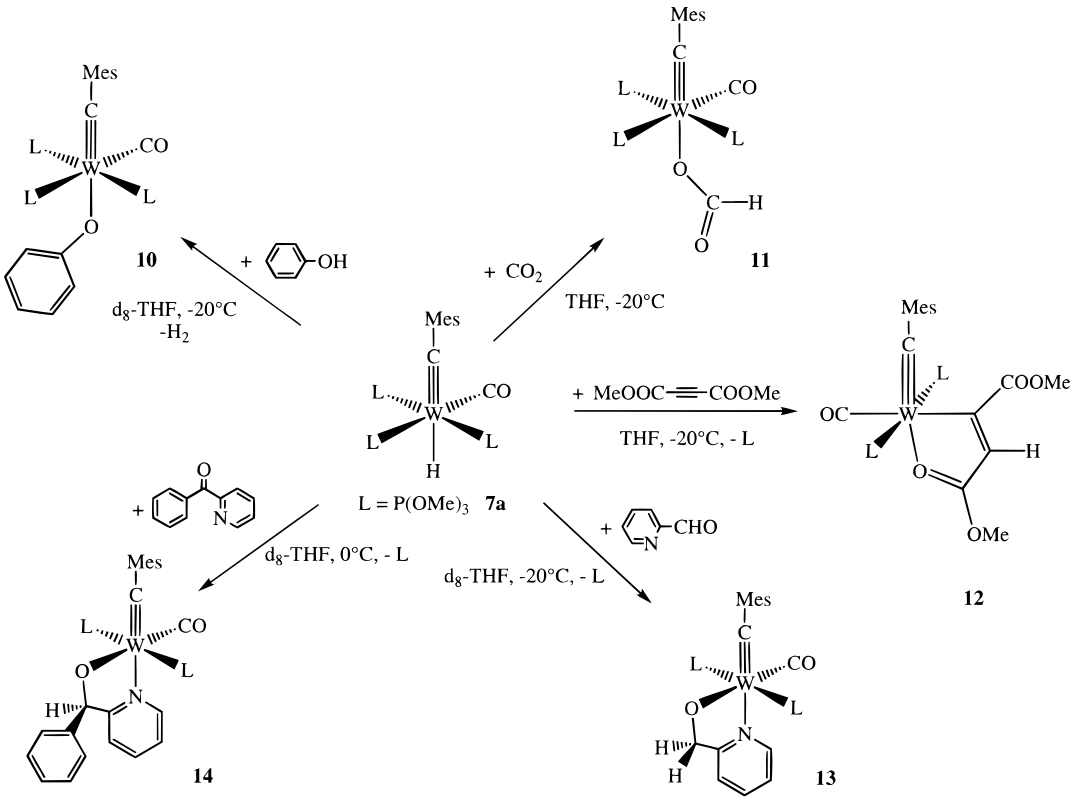


To increase the thermal stability of the carbyne hydride complex, a tridentate chelating ligand was introduced. **7d** is accessible from **5d** at −20 °C. However, warming to room temperature again causes decomposition of the tungsten hydride. We finally synthesized a carbyne hydride complex with four phosphorus donors in the coordination sphere, **8a**. Although this compound too cannot be handled at room temperature without decomposition, experiments indicate that **8a** is indeed more stable than **7a**. We will return to this fact at a later point of our discussion.

The structures of the four tungsten hydride complexes **7a**,**b**,**d** and **8a** were assigned by NMR spectroscopy. The chemical shifts for the hydride ligands are in the range from −4.6 to −6.2 ppm. For **7a**,**d**, the signals appear as a quartet, since the small difference in $J_{HP^{t\text{-}CO}}$ and $J_{HP^{t\text{-}P}}$ could not be resolved in the experiments. For **7b**, the expected splitting into a doublet of a triplet is observed, and for **8a**, the four phosphorus donors split the hydride signal into a quintet. $^{31}P\{^1H\}$ NMR spectroscopy unequivocally establishes the coordination geometry of the phosphorus donors.

**Reactivity studies of *trans*-W(CMes)(CO)H(P(OMe)$_3$)$_3$.** The reaction patterns of the new class of carbyne hydride complexes have been investigated for *trans*-W(CMes)(CO)H(P(OMe)$_3$)$_3$ (**7a**). Selected transformations are collected in Scheme 6.

To establish experimentally the hydridic polarization of the tungsten−hydrogen bond, **7a** was reacted with a weak acid. When a solution of W(CMes)(CO)H(P(OMe)$_3$ and excess phenol is kept for 4 days at −20 °C, the complete consumption of **7a** is observed, and compound **10** is detected with a spectroscopic yield of 60%. This complex results from protonation of the transition-metal complex and subsequent loss of dihydrogen. The evolution of $H_2$ can also be traced in the proton NMR spectrum. The formation of the phenolate complex **10** thus indicates substantial hydridic character of the W−H functionality in **7a**.

We further investigated the reduction potential of the prototype **7a** toward carbon dioxide and unsaturated organic compounds, such as acetylenes, aldehydes, and ketones. The reaction with $CO_2$ proceeds smoothly, and after a reaction time of 1 h, complex **11** is formed in good yield. Two isomers can possibly result as insertion products, namely a hydroxycarbonyl complex, [M]−COOH, or a formate complex, [M]−OCHO. In the literature, formate complexes are reported almost exclusively,[15] and **11** is yet another representative of this class of compounds. This is concluded from the IR spectra,[16] as well as from the small value of the $^3J_{PC}$ coupling constant of the formate ligand. Two $\nu$(CO) bands in the infrared spectrum are assigned to the carbonyl group (1946 cm$^{-1}$) and to the formate ligand (1633 cm$^{-1}$). In the $^{13}C\{^1H\}$ NMR spectrum, the resonance at 167.1 ppm is assigned to the C formate nucleus. Coupling with the P atoms splits this signal into a doublet of a triplet, with values for $^3J_{PC}$ of 6.2 and 1.5 Hz. The relatively large difference in the coupling constants is indicative of a strong distortion from an octahedral coordination geometry around the tungsten center. In contrast, $^2J_{PC}$ of the metal bonded carbon atom of a hydroxycarbonyl ligand can be expected at much higher values.

When a solution of **7a** in THF is reacted with the symmetrically substituted acetylene MeOOCC≡CCOOMe

(15) (a) Darensbourg, D. J.; Kudaroski, R. A. *Adv. Organomet. Chem.* **1983**, *22*, 129. (b) Sneeden, R. P. A. In *Comprehensive Organometallic Chemistry;* Wilkinson, G., Stone, F. G. A., Abel, E. W., Eds.; Pergamon: Oxford, U.K., 1982; Vol. 8, Chapter 50.4.

(16) Hillhouse, G. L.; Haymore, B. L. *Inorg. Chem.* **1987**, *26*, 1876.

for 24 h at −20 °C, the *trans* insertion product **12** is obtained in a clean reaction. Its structure has been determined by NMR and IR spectroscopy and is confirmed by mass spectrometry. In the $^{31}P\{^1H\}$ spectrum, the chemically equivalent P atoms are detected at 160.9 ppm. This signal shows tungsten satellites with a value for $^1J_{PW}$ of 433 Hz, characteristic for $P(OMe)_3$ ligands in *trans* positions.[17] The spectroscopic data of the organic ligand are similar to those published for the analogous product of the reaction between the isoelectronic nitrosyl compound[18] *trans*-$W(CO)_2H(NO)(PMe_3)_2$ and MeOOCC≡CCOOMe. **12** does not directly result from the insertion of the acetylene into the W−H bond but is formed via subsequent isomerization of the primary insertion product **12a**.

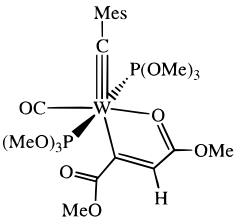


**12a**

If the reaction between **7a** and the acetylene is carried out at −60 °C, **12a** can be detected by NMR spectroscopy. When the reaction mixture is warmed to −20 °C, complex **12** is formed within 1 day. A similar situation was observed for the aforementioned nitrosyl hydride compound. In this case, however, the isomerization reaction is much slower, and both isomers could by characterized by X-ray structure determination.[18]

It was argued that the driving force for the isomerization reaction might be the fact that the $\pi$-donating oxygen substituent favors a coordination *trans* to the strongest $\pi$-accepting ligand.[18] If this argument holds true, the CR moiety indeed has to be looked at as a strong $\pi$-acceptor, which can even compete with CO.

The reduction of benzaldehyde with **7a** could not be achieved at the required reaction temperature of −20 °C, and even at 0 °C only decomposition could be observed. The reaction with more activated aldehydes was, however, successful. **7a** reacts with pyridine-2-carbaldehyde in THF at −20 °C within 24 h to form the insertion product **13** in 80% yield. **13** decomposes at room temperature; therefore, this complex was characterized by NMR spectroscopy. The two chemically equivalent P atoms appear in the $^{31}P\{^1H\}$ spectrum as a singlet at 148.8 ppm, with tungsten satellites, which exhibit a $^1J_{WP}$ coupling constant of 437 MHz. This value again is characteristic for two $P(OMe)_3$ ligands in *trans* positions.[17] The *ortho* H of the pyridine ring is detected as a doublet at 9.14 ppm. In comparison to the signal for the free ligand, this signal is shifted to lower field by 0.34 ppm, which is a consequence of the coordination of the pyridine nitrogen to the metal center. When the insertion is followed by NMR spectroscopy, the primary insertion product **13a** can be detected in the initial state of the reaction.

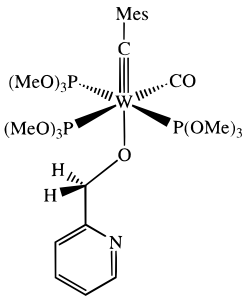


**13a**

In the $^{31}P\{^1H\}$ spectrum a characteristic system of doublet and a triplet resonance are seen at 158.5 and 154.4 ppm, respectively. For the triplet resonance, a $^2J_{PP}$ coupling constant of 46.7 Hz is measured.

The reaction of 2-benzoylpyridine with **7a** requires reaction temperatures around 0 °C and a reaction time of 48 h to afford the insertion product **14**. Since at this temperature decomposition of **7a** occurs as a side reaction, **14** is obtained in a yield of only 35%. This complex decomposes at room temperature. However, the compound could be identified by NMR spectroscopy, and the characteristic resonances show the same features as those measured for **13**. In contrast to **13**, no primary insertion product could be observed during the formation of **14**. A similar observation was made for the reaction of *trans*-$W(CO)_2H(NO)(PMe_3)_2$ with the activated ketone 2-benzoylpyridine.[18]

The insertion reactions, which have been presented here, do indeed indicate an enhanced reactivity of the tungsten−hydrogen bond. Reactions with $CO_2$, acetylenes, and activated carbonyl functionalities already take place at temperatures around −20 °C, whereas related nitrosyl complexes react only at elevated temperatures and generally require longer reaction times.[18] On the other hand, the thermal instability of the hydride complexes, which requires the low reaction temperature, might prevent reactions with more inert carbonyl functions and limits the scope of possible applications. The lability of the coordination sphere of **7a** might be one reason for the instability of this complex. In the next section, we present a series of experiments, which further support this hypothesis.

**Hydride Migration and Carbene Formation for $W(CMes)(CO)H(P(OMe)_3)_3$.** When **7a** is treated with the phosphorus donors $P(OMe)_3$ or $PMe_3$ at −50 °C, no exchange of carbon monoxide with phosphine ligands could be observed. Instead, new compounds appeared, which were identified as the carbene complexes $W(CHMes)(CO)(P(OMe)_3)_4$ (**15a**) and $W(CHMes)(CO)(PMe_3)_2(P(OMe)_3)_2$ (**15b**), respectively. Similarly, the reaction between carbon monoxide and **7a** did not result in an insertion of CO into the metal−hydride bond but produced the carbene complex **16** (Scheme 7).

The reaction between **7a** and 1−3 equiv of $P(OMe)_3$ at −20 to −80 °C led to an equilibrium between **15a** and **7a**, which was investigated by NMR spectroscopy. At low temperatures and large excess of the phosphorus donor, product formation was favored. On the other hand, at higher temperatures or smaller amounts of excess $P(OMe)_3$, the equilibrium lies on the side of the hydride complex **15a**, which clearly manifests itself in

(17) Verkade, J. G.; Quin, L. D. *Phosphorus-31 NMR Spectroscopy in Stereochemical Analysis*; VCH: Weinheim, Germany, 1987; Vol. 8.
(18) van der Zeijden, A. A. H.; Bosch, H. W.; Berke, H. *Organometallics* **1992**, *11*, 563.

**Scheme 7**

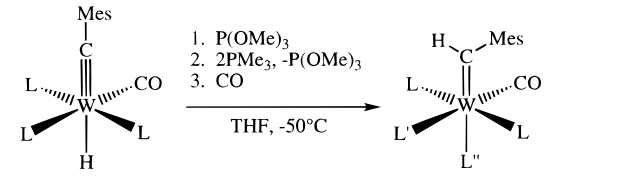


L = $P(OMe)_3$ **7a**

1. L' = L" = $P(OMe)_3$ **15a**
2. L' = L" = $PMe_3$ **15b**
3. L' = $P(OMe)_3$, L" = CO **16**

the NMR and IR spectra. Three characteristic signals are observed in the $^{31}P\{^1H\}$ spectrum. The resonance at 165.3 ppm, which belongs to $P^{t-CO}$, exhibits an unusually small $^1J_{PW}$ coupling constant of 235 Hz. The expected value for a $P^{t-CO}$ ligand in an octahedral coordination environment lies in the range between 340 and 380 Hz.[17] The small $^1J_{PW}$ value indicates a significant deviation of the angle $\angle(P^{t-CO}-W-C^{t-P})$ from the ideal value of 180°. We have observed a similar effect before and were able to correlate the small $^1J_{PW}$ value with geometric data obtained from an X-ray structure analysis.[19] The carbene proton appears in the $^1H$ NMR spectrum as a multiplet at 16.92 ppm. The characteristic value of 30.2 Hz for $P^{t-CH_2}$ can already be seen in this complex signal. Precise values for the $^3J_{HP}$ coupling constants have been determined by selective decoupling from the phosphorus nuclei.

To further establish the equilibrium between **7a** and **15a**, a 1D-SEXSY spectrum with NOE difference pulse sequence was recorded. Irradiating at the hydride resonance of **7a** indicated an exchange with the carbene proton of **15a**. Similarly, when irradiation was carried out at the carbene proton resonance, an inverted signal for the hydride ligand was detected. This experiment establishes that both H resonances are in exchange equilibrium and that on the NMR time scale a transition between **7a** and **15a** takes place.

In the $^{13}C\{^1H\}$ spectrum two signals at 287.2 and 219.5 ppm are observed. In a DEPT-135 experiment a positive signal at 287.2 ppm was obtained, whereas no resonance was seen at 219.5 ppm. Thus, the latter resonance stems from the carbonyl ligand, whereas the former signal belongs to the carbene moiety of **15a**.

The equilibrium reaction was also investigated by IR spectroscopy at −30 °C. In the $\tilde{\nu}$(CO) region, two bands appear at 1937 and 1803 $cm^{-1}$, belonging to **7a** and **15a**, respectively. A subsequent increase in $P(OMe)_3$ concentration led to an increase in intensity for the band at 1803 $cm^{-1}$, whereas the absorption at 1937 $cm^{-1}$ decreased. The opposite effect could be seen when the temperature in the IR cell was raised to 0 °C. This experiment establishes a migration of the hydride onto the carbyne ligand. Alternative reduction of the carbonyl group would result in a formyl ligand. This, however, is expected to cause a $\tilde{\nu}$(CHO) stretching frequency at wavenumbers much lower than those observed.

The reaction between **7a** and $PMe_3$ at -40 °C leads to the formation of the carbene complex **15b**. Both the carbonyl and the carbene ligand are identified by $^{31}C\{^1H\}$ spectroscopy. In the $^{31}P\{^1H\}$ spectrum, the signal at 150.9 ppm is split into a doublet of a doublet, whereas the resonances at −38.3 and −38.9 ppm appear as triplets of a doublet. This indicates that in **15b** two $P(OMe)_3$ and two $PMe_3$ ligands are present. The two equivalent phosphite groups are *trans* to each other, whereas the two trimethylphosphine ligands are *trans* to the two $\pi$-accepting moieties. In contrast to **15a**, complex **15b** is not in equilibrium with the carbyne hydride **7a**.

In a similar fashion, treatment of a solution of **7a** in THF with CO gas at −50 °C results in the new compound **16**. It can be stored in solution at −20 °C but decomposes within minutes at room temperature. As was the case for **15b,** this complex is not in equilibrium with **7a**.

Two $\tilde{\nu}$(CO) stretching frequencies at 2001 and 1877 $cm^{-1}$ are observed in the IR spectrum, pointing to two carbonyl ligands in a *cis* arrangement. The $^{31}P\{^1H\}$ spectrum reveals that three $P(OMe)_3$ ligands coordinate in a meridional fashion. The small $^1J_{PW}$ coupling constant of 230 Hz for the ligand *trans* to the carbonyl group again indicates a significant distortion from an idealized octahedral geometry. The carbene proton appears as a quartet at 16.36 ppm with identical $^3J_{HP}$ coupling constants of 4.3 Hz for all three P nuclei. Therefore, the carbene group is *cis* to all three phosphite ligands, and consequently the two carbonyl groups must be located *trans* to the carbene moiety and to one $P(OMe)_3$ ligand, respectively. When the reaction between **7a** and carbon monoxide is carried out with $^{13}CO$, after a short time a signal at 207.8 ppm appears in the $^{13}C\{^1H\}$ NMR spectrum. This doublet of a triplet resonance shows small $^2J_{CP}$ coupling constants of 7.8 and 11.3 Hz, which allows one to conclude that the incoming $^{13}CO$ selectively coordinates *trans* to the carbene ligand.

In the proton NMR spectrum of **16**, an additional weak signal is found in the region for a carbene ligand. It appears as a doublet at 17.05 ppm with a coupling constant $^3J_{HP}$ of 34.6 Hz. This value is indicative of a P ligand *trans* to the proton. The low intensity of this resonance, however, prohibits a more detailed analysis of this signal.

We should further mention the fact that neither for **7d** nor for **8a**, in the presence of excess $P(OMe)_3$, could the formation of a carbene complex be spectroscopically detected. Also, both hydrides do not show any reactivity toward carbon monoxide, as was detected for compound **7a**.

From all the observations described above, we might draw the picture for hydride migration and carbene formation shown in Scheme 8.

The reaction sequence is initialized by dissociation of one $P(OMe)_3$ ligand to form a five-coordinated intermediate. Several experimental facts support this assumption. In any solution of **7a**, free $P(OMe)_3$ can always be detected in the NMR spectra. This indicates the lability of one of the phosphorus donors toward dissociation. The fact that no carbene formation is observed when **7d** is treated with CO or excess $P(OMe)_3$ at −10 °C provides further support for our assumption. The tridentate dppe ligand substantially stabilizes the P coordination sphere in **7b**, and ligand dissociation is not a facile process any more. The five-coordinate carbyne intermediate possesses a free coordination site, but not a hydride ligand, *trans* to the carbyne group. Coordination of excess phos-

(19) Baur, J.; Jacobsen, H.; Burger, P.; Artus, G.; Berke, H. *Eur. J. Inorg. Chem.* **2000**, 1411.

**Scheme 8**

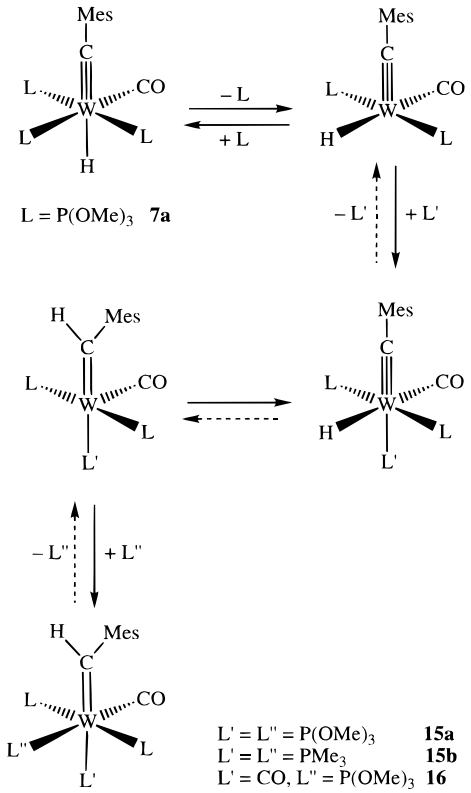


phorus donor or CO leads to an octahedral complex with $H^-$ and CR in *cis* positions. If two different phosphorus donors are present, for example $P(OMe)_3$ and $PMe_3$, we can assume that the stronger $\sigma$-donor will preferentially coordinate to the transition-metal fragment. In the next step, hydride migration onto the carbyne moiety takes place, leading to a five-coordinated carbene fragment. Coordination of another ligand molecule then completes the formation of the complexes **15a**,**b** and **16**. Since **15a** is in equilibrium with **7a**, all steps in the reaction sequence leading to **15a** must be at equilibrium as well. In contrast, during the formation of **15b** or **16**, at least one of the steps discussed in Scheme 8 must be irreversible or represent a chemical equilibrium, which lies almost exclusively on the product side.

Although the mechanism presented in Scheme 8 is consistent with the experimental observations and explains the stereochemistry observed for the reaction products, the considerations regarding the geometry of the five-coordinated intermediates are hypothetical and are not supported by experimental facts. In connection with this problem, for the formation of **16**, we cannot tell at which point in the reaction sequence carbon monoxide is coordinating to the transition-metal fragment, although we know that in the final product the incoming CO is found *trans* to the CR group. The carbene formation step via direct migration of $H^-$ onto the CR group requires a *cis* arrangement of these two ligands. However, alternative migration routes, which do not require an isomerization of the carbyne complex and might involve formyl intermediates, cannot definitely be excluded. To obtain further information on the carbene formation process, we have performed a computational study on the model complexes $W(CH)(CO)H(PH_3)_3$ (**I**) and $W(CH)H(PH_3)_4$ (**XV**), which will be discussed in the next section.

**Theoretical Investigation of the Carbene Formation Reaction.** In Figure 1, the energetic profiles of various possible pathways for the formation of the

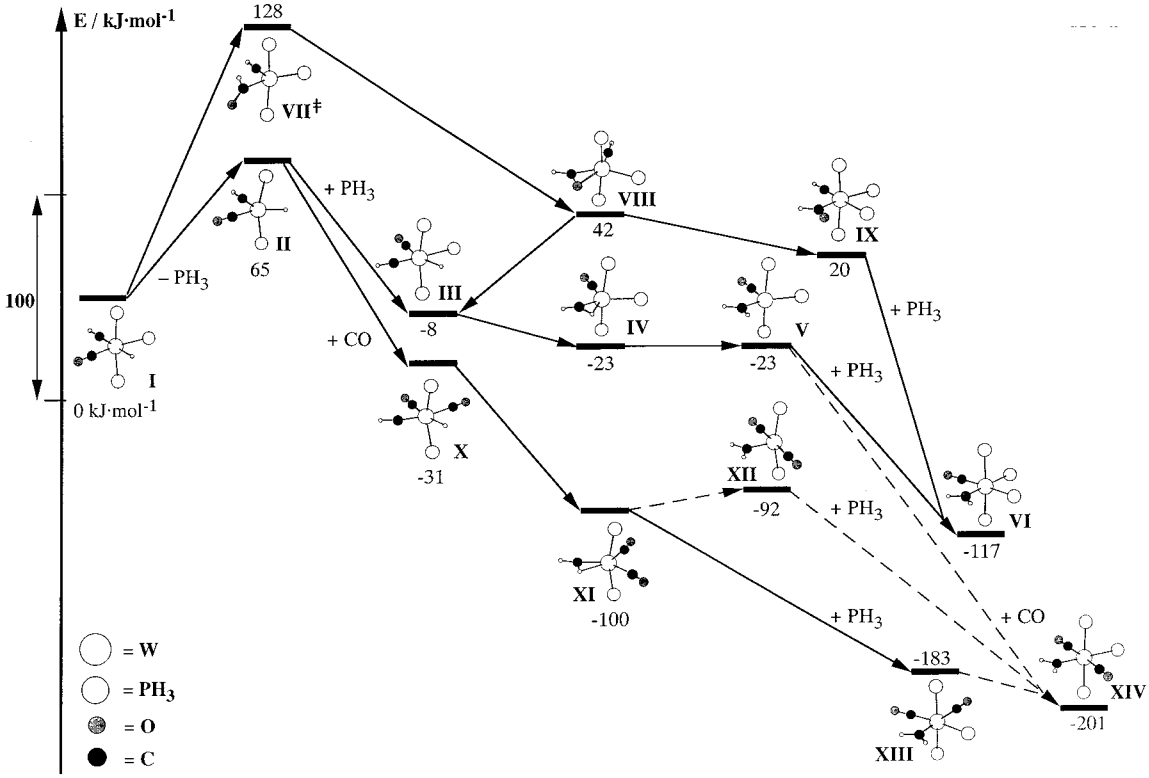


**Figure 1.** Possible reaction pathways for the formation of the carbene complexes **VI** and **XIII** from $W(CH)(CO)H(PH_3)_3$ **(I),** as obtained from density functional calculations.

carbene species $W(CH_2)(CO)(PH_3)_4$ (**VI**) and $W(CH_2)(CO)_2(PH_3)_3$ (**XIII**) are displayed.

All reaction routes originate from the model complex **I**, which, together with the free ligands that dissociate or coordinate during the course of the reaction, is taken as the reference system at zero energy. Although not explicitly indicated, all energy differences are taken for systems containing the same number of atoms, including coordinated as well as free ligands.

The dissociative pathway is initiated by loss of the phosphine ligand *trans* to the carbonyl group, leading to the five-coordinated species $W(CH)(CO)H(PH_3)_2$ (**II**). In the most stable isomer, the remaining two $PH_3$ ligands are located *trans* to each other, while the *cis* geometry **IIa** is calculated to be 9 kJ/mol higher in energy. The *trans* arrangement of the P ligands will be maintained during the whole course of the calculated reaction. System **II** is 65 kJ/mol higher in energy than the reference system **I.** To judge whether the dissociation step is facile or not, we have to keep in mind that our calculated results correspond to differences in total bonding energies. Approximating entropy changes from translational and rotational contributions as 50 kJ/mol at −25 °C, and taking the correction to the internal energy as 4 kJ/mol, obtained from an approximate value of 400 $cm^{-1}$ for $\tilde{\nu}$(WP), we can estimate a $\Delta G$ value of about 11 kJ/mol for the ligand dissociation step. Thus, the generation of the five-coordinated intermediate **II** is not a critical step in the carbene formation. This conclusion is in accord with the experimental observation that, in any solution of **7a**, free phosphine ligand is present. The loss of a carbonyl group results in the complex **IIb**, which is 142 kJ/mol higher in energy, and does not represent a feasible entry into the reaction sequence.

Recoordination of the phosphine ligand might lead to back-reaction to **I** or result in the formation of complex **III,** in which now the carbyne and the hydride ligand are *cis*. This compound is 8 kJ/mol more stable than **I.** The P ligand *trans* to the CH group displays an unusually long *d*(W−P) bond length of 2.65 Å, about 0.2 Å longer than for the other two phosphines. At the same time, the distance *d*(W−CH) gets shorter in the isomerization process **I** → **III**. This indicates an increase in metal−carbyne bond strength, which might provide a driving force for the iomerization reaction.

Hydride migration onto the CH group leads to the carbene species **IV**, which possesses an interesting coordination geometry.

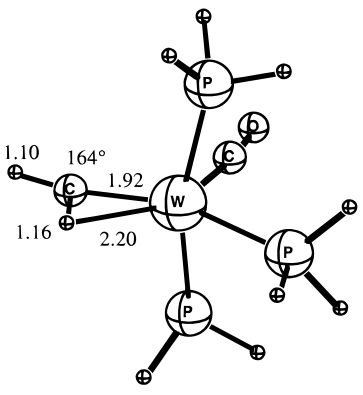


**IV**

The carbene ligand pivots in place so that one small and one large W−C−H angle with values of 88 and 164° are seen. One of the C−H bond lengths is, at 1.16 Å, substantially elongated. The same H atom comes close to the metal center, and the short distance *d*(W−H) of 2.20 Å indicates some additional bonding interaction. Thus, one might describe the carbene ligand in **IV** as $\eta^2$-$CR_2$. The distorted $\eta^2$-coordination mode has first been observed for alkylidene complexes of electron-deficient transition metals.[20] A molecular orbital analysis[21] of these molecules traces the deformation to an intramolecular electrophilic interaction of acceptor orbitals of the metal with the carbene lone pair. A secondary interaction weakens the C−H bond and attracts the H atom to the metal center. Similar orbital interactions are at work in the present case. We will return to $\eta^2$-carbene coordination once more in the last section of our discussion.

The migration step **III** → **IV** is energetically favorable by 15 kJ/mol. The open form **V,** however, is virtually isoenergetic with **IV** and possesses a free coordination opposite to the carbene ligand. Uptake of another $PH_3$ then leads to the final product $W(CH_2)(CO)(PH_3)_4$ (**VI**).

An alternative reaction route toward **VI** might involve migration of the hydride onto the carbonyl group, leading to the formation of the tungsten formyl **VIII**. In this complex, the CHO group is bonded side-on in $\eta^2$ fashion, with the H atom being *cis* to the carbyne group. The formation of **VIII** requires an activation energy of 128 kJ/mol. In the transition state **VII**$^{\ddagger}$, an $\eta^1$ -formyl group is located in the plane of the three P donor ligands. The five-coordinated formyl species is 42 kJ/mol higher in energy than the reference system and might rearrange to the more stable compound **III**. Alternatively, coordination of a $PH_3$ group leads to the formyl compound **IX**, from which the final product **VI** can be reached by H transfer from the formyl onto the carbyne moiety. **IX** is 20 kJ/mol higher in energy than **I,** and the very long *d*(W−P) separation of 2.72 Å indicates that the P ligand *trans* to CH is only weakly bonded. The high activation barrier for the formation of the $\eta^2$ intermediate, as well as the unfavorable relative energies of the CHO complexes **VIII** and **IX**, suggests that formyl complexes do not occur in the course of the carbene formation.

When both carbon monoxide and phosphorus donors are present in the reaction mixture, the intermediate **II** coordinates CO to form *cis*-$W(CH)(CO)_2H(PH_3)_2$ (**XI**). This complex is 23 kJ/mol more stable than **III,** which suggests that in the formation of **XIII**, CO coordination preferably occurs before $PH_3$ coordination. The incoming CO group is situated *trans* to the carbyne ligand. The coordination of the CH group in **X** is not linear but shows a W−C−H angle of 163°, anticipating the coordination mode of a $\eta^2$-carbene unit. The formation of a complex **XI** containing such a ligand is energetically favorable by 69 kJ/mol. The symmetric coordination geometry **XII** is 8 kJ/mol higher in energy. When a P donor attacks **XI** such that cleavage of the agostic inter-

(20) (a) Churchill, M. R.; Youngs, W. J. *J. Chem. Soc., Chem. Commun.* **1978**, 1048. (b) Shultz, A. J.; Williams, J. M.; Schrock, R. R.; Rupprecht, G. A.; Fellmann, J. D. *J. Am. Chem. Soc.* **1979**, *101*, 1593.

(21) Goddard, R. J.; Hoffmann, R.; Jemmis, E. D.. *J. Am. Chem. Soc.* **1980**, *102*, 7667.

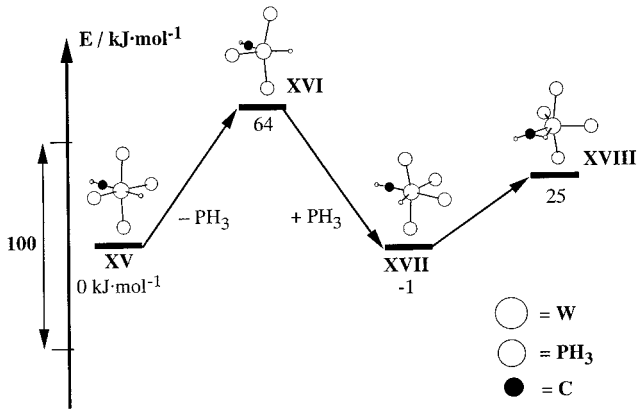


**Figure 2.** Calculated energy profile for ligand isomerization and carbene formation for $W(CH)H(PH_3)_4$ (**XV**).

action and formation of the new W−P bond occur in a concerted fashion, the product **XIII** is formed in a way that the new CO ligand ends up *trans* to the carbene group, in accordance with the experimental observations.

Complex **XIII** is not the most stable $W(CH_2)(CO)_2(PH_3)_3$ isomer. Compound **XIV**, having the CO as well as the $PH_3$ groups *trans* to each other, is more stable by 18 kJ/mol. Although the *trans* arrangement of the carbonyl ligands seems energetically unfavorable, this coordination modes ensures that the strongest $\pi$ acceptor in the system, namely the $CH_2$ ligand, does not have to share electron density from an occupied metal-based d orbital with a CO group. A shortening in the $d$(W−$CH_2$) bond distance by 0.02 Å in the process **XIII** → **XIV** indicates an increase in the carbene bond strength. Thus, **XIII** is the kinetic product of the carbene formation reaction, whereas **XIV** represents the thermodynamic product. The additional signals in the $^1$H NMR spectrum of **16** might belong to such a species, which also possesses a phosphorus donor *trans* to the carbene ligand. Alternative routes to complex **XIV** might involve the regular carbene intermediate **XII**, or system **V,** if $PH_3$ coordination precedes CO coordination.

We now turn to complex $W(CH)H(PH_3)_4$ (**XV**), a model system for compound **8a**. We recall that for **8a**, the formation of a carbene complex could not be observed.

The computed energy profile for carbene formation via ligand dissociation for **XV** is displayed in Figure 2. The calculations indicate that both the *trans* and the *cis* isomers of $W(CH)H(PH_3)_4$ should be of equal energy. Here, we have to keep in mind that the real $P(OMe)_3$ ligands possess greater steric requirements than the small model ligand $PH_3$. In the isomerization reaction **I** → **III** the steric influence of the P donors is only of secondary importance, since the main coordination geometry of the P framework is maintained. Steric effects will be of importance for the reaction **XV** → **XVI**, since now a rearrangement of the phosphine ligands takes place. It is reasonable to assume that **XVI** is energetically disfavored on steric grounds.

The changes in energy associated with hydride migration are crucial for the carbene formation process. Establishing the $\eta^2$-carbene complex **XVIII** requires an energy of 26 kJ/mol; the symmetric $CH_2$ compound **XVIIIa** is even 35 kJ/mol higher in energy. The four phosphorus donors in **XVI** render the metal center relatively electron rich, and the carbyne ligand is the only $\pi$-accepting group present in the molecule. Carbene formation reduces the $\pi$-accepting power of the C-based ligand and is therefore energetically not a favorable process.

Our model calculations indicate that formation of complex **15a** is likely to proceed via a dissociative mechanism and does not involve formyl complexes. In the formation of **16a**, coordination of the CO group precedes coordination of a phosphorus donor. This leads to a complex with the incoming CO *trans* to the carbene and the two carbonyl groups in a *cis* arrangement. The hydride migration is facilitated by the presence of a CO group in the coordination sphere of the complex. Compound **8a** does not isomerize into to a carbene complex, since formation of the $\eta^2$-CHR intermediate is energetically disfavored.

**Carbene Formation via Protonation Reactions.** We conclude our discussion by briefly commenting on an alternative transformation of carbyne complexes into carbene compounds. Treatment of the carbyne chlorides *trans*-$W(CR)(Cl)L_4$ with HCl results in carbene complexes of the type $W(CHR)(Cl)_2L_3$. These reactions were first described by Schrock[22] and Mayr.[9a] X-ray structure determinations[9a,23] of the tungsten carbenes revealed the presence of an $\eta^2$-CHR group, as discussed in the previous section. In a recent neutron diffraction study[24] of $W(CHMe)Cl_2(CO)(PMe_3)$, the precise coordination geometry of the carbene moiety could be determined. The bond distances $d$(W−H) and $d$(C−H) amount to 1.922(6) and 1.185(7) Å, and the W−C−H angle is 74.7(3)°. The structural deformation for the $d^4$ complexes can again be explained by enhanced orbital interaction of the carbene lone pair with the metal center.[21] In addition, the C−H $\sigma$ orbital acts as a $\sigma$ donor toward the metal center. Because of this agostic interaction, Mayr describes the bond between the alkylidene group and metal center even as a triple bond.[24]

In an analogous fashion, the reaction of **3a** with HCl at room temperature furnishes the carbene complex **17**, which can be isolated as a red, crystalline material (Scheme 9).

**Scheme 9**

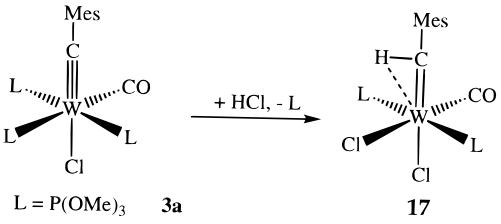


L = $P(OMe)_3$ **3a** **17**

Although **17** could not be characterized in the solid state, NMR spectroscopy clearly reveals the $\eta^2$-coordination of the CHMes group. The carbene proton appears at −0.38 ppm as a triplet with a coupling constant $^3J_{HP}$ of 4.8 Hz. In addition, tungsten satellites are observed with a $^1J_{HW}$ coupling of 28.7 Hz. This indicates that the

(22) Wengrovius, J. H.; Schrock, R. R.; Churchill, M. R.; Wassermann, H. J. *J. Am. Chem. Soc.* **1982**, *104*, 1739.
(23) Churchill, M. R.; Wassermann, H. J. *Inorg. Chem.* **1983**, *22*, 1574.
(24) Bastos, C. M.; Lee, K. S.; Kjelsberg, M. A.; Mayr, A.; Vaan Engen, D.; Koch, S. A.; Franolic, J. D.; Klooster, W. T.; Koetzle, T. F. *Inorg. Chim. Acta* **1998**, *279*, 7.

interaction between the carbene proton and the metal center is present not only in the crystal but also in solution. Weakening of the C−H bond results in a very small $^1J_{HC}$ coupling constant of 75.2 Hz, which provides further evidence for the agostic interaction.

## Conclusion

In this work, we have introduced a new class of activated transition-metal hydride complexes, namely tungsten carbyne hydrides of the type *trans*-W(CMes)-$(CO)_nHL_{4-n}$. We have developed a synthetic route which provides access to a wide variety of hydride complexes. In this context we also described the synthesis of the chloride complexes *trans*-W(CMes)$(CO)_n(Cl)L_{4-n}$ and borate adducts W(CMes)$(\eta^2$-$H_2BH_2)(CO)_nL_{3-n}$. Prototypical reactivity studies revealed both the great potential and the drawbacks of these new compounds. Complex **7a** already reacts at low temperatures with unsaturated organic compounds and displays an enhanced reactivity compared to the related nitrosyl derivative *trans*-$W(CO)_2H(NO)(PMe_3)_2$. On the other hand, low temperatures are required in order to prevent decomposition of the hydride complex, thus limiting the scope of its potential application as a hydrogenation reagent. Only activated aldehydes such as pyridine-2-carbaldehyde undergo a reaction with **7a** before decomposition sets in. One reason for the thermal instability of the hydride complexes is the labile coordination sphere of the phosphorus donors, which leads to hydride migration and carbene formation as one of the decomposition pathways for **7a**. Our studies have shown that strategies to increase the stability of the phosphorus framework include the use of chelating ligands, as well as the replacement of carbonyl ligands by additional phosphorus donors. Stronger $\sigma$-donating P-ligands should further stabilize the complexes and, at the same time, lead to an even more reactive W−H functionality. This could be concluded from the reactivity patterns of the borate adducts **5a**,**b.** Following these considerations, and utilizing the synthetic methodology that we have developed in this work, we have already designed a rational synthesis for the compound *trans*-W(CMes)-$(dmpe)_2H$.[25] This complex is indeed stable at room temperature and could be characterized by an X-ray structure analysis. Preliminary reactivity studies revealed its high activity in hydrogen transfer reactions.[25a] Further studies on this promising complex as well as on related nitrosyl derivatives are currently under way in our laboratories.

## Experimental Section

All manipulations were performed under a nitrogen atmosphere using standard Schlenk techniques. Solvents were dried according to standard procedures and distilled under $N_2$ prior to use. $PMe_3$[26] and $[W(C(O)Mes)(CO)_5][N(CH_3)_4]$[8] were synthesized following slightly modified[27] literature procedures, whereas all other reagents were purchased and used without further purification. The following instruments were used for spectroscopic and physical characterization: Varian Gemini 200 and Gemini 300 NMR spectrometers ($^1$H and $^{13}$C chemical shifts are referred to TMS and referenced through the residual proton or $^{13}$C resonances of the deuterated solvent; $^{31}$P chemical shifts were externally referenced to 85% $H_3PO_4$); Bio-Rad FTS-45 IR spectrometer; Finnigan/MAT 8320 mass spectrometer; LECO CHNS-932 for elemental analyses.

***trans*-W(CMes)Cl(CO)$_2$(py)$_2$ (1).** $[W(C(O)Mes)(CO)_5]$-$[N(CH_3)_4]$ (6.83 g, 12.5 mmol) was dissolved in $CH_2Cl_2$ (150 mL) and cooled to −100 °C. Oxalyl chloride, $C_2O_2Cl_2$ (1.3 mL, 15 mmol), in $CH_2Cl_2$ (20 mL) was precooled and added. The reaction mixture immediately turned black and was stirred for 30 min at −80 °C. A vivid gas evolution could be observed. The yellow suspension was further stirred at 0 °C for another 30 min, during which time the gas evolution came to an end. The suspension was cooled to −40 °C, and pyridine (8.0 mL, 100 mmol) was added. The mixture was warmed to room temperature and stirred overnight. Filtration through Celite and evaporation of the reaction mixture afforded the dark orange crude product, which was washed with hexane (2 × 20 mL). Recrystallization from $CH_2Cl_2$/hexane yielded **1** as an orange powder (6.76 g, 12.0 mmol, 95%). IR (KBr, cm$^{-1}$): 1976 (s), 1889 (s). $^1$H NMR (200 MHz, $CDCl_3$, ppm): 9.09 ("d", 4H, *o*-py), 7.78 ("t", 2H, *p*-py), 7.29 ("t", 4H, *m*-py), 6.75 (s, 2H, Mes), 2.43 (s, 6H, C*H*$_3$-Mes), 2.20 (s, 3H, C*H*$_3$-Mes). $^{13}$C{$^1$H} NMR (50.3 MHz, $CDCl_3$, ppm): 266.9 (s, *C*Mes), 221.9 (s, CO), 153.2 (s, *o*-py), 144.1 (s, ipso-Mes), 140.8 (s, *o*-Mes), 138.2 (s, *p*-py), 137.6 (s, *p*-Mes), 128.1 (s, *m*-Mes), 124.9 (s, *m*-py), 21.3 (s, *C*H$_3$-Mes), 20.5 (s, 2*C*H$_3$-Mes). MS (FAB-Neg, LM = $CH_2Cl_2$, M = NBOH, *m*/*z*, %): 564 ($M^+$, 20), 538 ($M^+$ − CO, 30), 508 ($M^+$ − 2 CO, 50), 487 ($M^+$ − py, 50), 457 ($M^+$ − py − CO, 60), 429 ($M^+$ − py − 2 CO, 80). A satisfactory elemental analysis could not be obtained.

***trans*-W(CMes)Cl(CO)$_2$(P(OMe)$_3$)$_2$ (2a).** According to the procedure described for **1,** a solution of $W(CMes)Cl(CO)_4$ (2.45 mmol) in $CH_2Cl_2$ was prepared. At −40 °C, $P(OMe)_3$ (0.63 mL, 5.37 mmol) was added. The mixture was warmed to room temperature, and CO evolution was observed. The solution was stirred overnight, and the solvent removed in vacuo. The dark yellow crude product was recrystallized from hexane. This afforded **2a** (1.40 g, 2.13 mmol, 87%), as a yellow oil at room temperature. IR (hexane, cm$^{-1}$): 2021 (s), 1960 (s). $^1$H NMR (300 MHz, $C_6D_6$, ppm): 6.57 (s, 2H, Mes), 3.51−3.47 (m, 18H, $P(OMe)_3$), 2.67 (s, 6H, C*H*$_3$-Mes), 1.96 (s, 3H, C*H*$_3$-Mes). $^{13}$C-{$^1$H} NMR (75.4 MHz, $C_6D_6$, ppm): 265.8 (t, $^2J_{CP}$ = 15.0 Hz, *C*Mes), 209.8 (dd, $^2J_{CP}$ = 87.0 × 30.5 Hz, CO), 144.7 (s, *ipso*-Mes), 141.7 (t br, *o*-Mes), 138.1 (s, *p*-Mes), 128.3 (s, *m*-Mes), 52.1 ("t", $P(OMe)_3$), 21.3 (s, *C*H$_3$-Mes), 20.8 (s, 2*C*H$_3$-Mes). $^{31}$P-{$^1$H} NMR (121.5 MHz, $C_6D_6$, ppm): 142.4 (s, $^1J_{PW}$ = 390 Hz). A satisfactory elemental analysis could not be obtained.

***trans*-W(CMes)Cl(CO)$_2$(PMe$_3$)$_2$ (2b).** A mixture of **1** (1.3 g, 2.13 mmol) and $PMe_3$ (0.51 mL, 4.70 mmol) in THF (150 mL) was stirred for 2 h at room temperature. The color changed from orange to yellow. After filtration through Celite, the dark yellow filtrate was evaporated in vacuo, and the crude product was washed with a small amount of hexane. Recrystallization from $CH_2Cl_2$/hexane yielded **2b** (1.09 g, 1.96 mmol, 92%) as a yellow powder. Analytically pure **2b** was obtained by recrystallization from $Et_2O$ at −30 °C. IR (KBr, cm$^{-1}$): 1989 (s), 1913 (s). $^1$H NMR (300 MHz, $d_8$-THF, ppm): 6.70 (s, 2H, Mes), 2.52 (s, 6H, C*H*$_3$-Mes), 2.12 (s, 3H, C*H*$_3$-Mes), 1.63 (m, 18H, $PMe_3$). $^{13}$C{$^1$H} NMR (75.4 MHz, $d_8$-THF, ppm): 267.5 (t, $^2J_{CP}$ = 9.7 Hz, *C*Mes), 215.7 (dd, $^2J_{CP}$ = 37.4 × 18.7 Hz, CO), 145.7 (s, ipso-Mes), 140.3 (s, *o*-Mes), 137.6 (s, *p*-Mes), 128.8 (s, *m*-Mes), 21.6 (s, 2*C*H$_3$-Mes), 21.4 (s, *C*H$_3$-Mes), 19.2 (m, $PMe_3$). $^{31}$P{$^1$H} NMR (121.5 MHz, $d_8$-THF, ppm): −28.5 (s, $^1J_{PW}$ = 238 Hz). MS (FAB-Neg, LM = $CH_2Cl_2$, M = NBOH, *m*/*z*, %): 558 ($M^+$, 2), 530 ($M^+$ − CO, 28), 524 ($M^+$ − Cl, 20), 502 ($M^+$ − 2 CO, 100). Anal. Calcd for $C_{18}H_{29}ClO_2P_2W$ (558.68): C, 38.70; H, 5.23. Found: C, 38.77; H, 5.24.

***trans*-W(CMes)Cl(CO)(py)(P(O$^i$Pr)$_3$)$_2$ (2c).** A solution of **1** (0.82 g, 1.45 mmol) and $P(OiPr)_3$ (3.3 mL, 14.5 mmol) in THF (80 mL) was refluxed for 16 h. The yellow-green solution was

(25) (a) Furno, F.; Bannwart, E.; Berke, H. *Chimia* **1999**, *53*, 350. (b) Furno, F.; Fox, T.; Schmalle, H. W.; Berke, H. *Organometallics* **2000**, *19*, 3620.

(26) Wolfsberger, W.; Schmidbaur, H. *Synth. React. Inorg. Met.-Org. Chem.* **1974**, *4*, 149.

(27) Bannwart, E. Ph.D. Thesis, Universität Zürich, 1998.

cooled and filtered through Celite, and the clear red filtrate was evaporated in vacuo. Recrystallization from hexane yielded **2c** (1.14 g, 1.30 mmol, 90%) as a red powder. IR (KBr, $cm^{-1}$): 1870 (s). $^1H$ NMR (300 MHz, $C_6D_6$, ppm): 9.52 ("d", 2H, *o*-py), 6.87 ("t", 1H, *p*-py), 6.74 (s, 2H, Mes), 6.58 ("t", 2H, *m*-py), 5.11 (m, 6H, PC*H*$(CH_3)_2$), 2.79 (s, 6H, C*H*$_3$-Mes), 2.06 (s, 3H, C*H*$_3$-Mes), 1.19 (m, 36H, PCH(C*H*$_3$)$_2$). $^{13}C\{^1H\}$ NMR (75.4 MHz, $CD_2Cl_2$, ppm): 262.6 (t, $^2J_{CP}$ = 17.0 Hz, $^1J_{CW}$ = 197.4 Hz, *C*Mes), 240.1 (t, $^2J_{CP}$ = 8.1 Hz, $^1J_{CW}$ = 168.8 Hz, CO), 155.7 (s, *o*-py), 145.7 (s, ipso-Mes), 141.0 (s, *o*-Mes), 137.0 (s, *p*-py), 135.4 (s, *p*-Mes), 127.8 (s, *m*-Mes), 123.3 (s, *m*-py), 68.8 (s, P*C*H$(CH_3)_2$), 24.3 (s, PCH(*C*H$_3$)$_2$), 21.5 (s, *C*H$_3$-Mes), 21.3 (s, 2*C*H$_3$-Mes). $^{31}P\{^1H\}$ NMR (121.5 MHz, $C_6D_6$, ppm): 145.1 (s, $^1J_{PW}$ = 438 Hz). MS (FAB-Neg, LM = $CH_2Cl_2$, M = NBOH, *m*/*z*, %): 795 ($M^+$ − py, 10), 768 ($M^+$ − CO − py, 22), 731 ($M^+$−CO − Cl − py, 3), 667 ($M^+$ − P(OiPr)$_3$, 25). Anal. Calcd for $C_{34}H_{58}NClO_7P_2W$ (874.09): C, 46.72; H, 6.69; N, 1.60. Found: C, 46.22; H, 6.51; N, 1.47.

***trans*-W(CMes)Cl(CO)$_2$(PPh$_3$)$_2$ (2d).** According to the procedure described for **1,** a solution of W(CMes)Cl(CO)$_4$ (6.66 mmol) in $CH_2Cl_2$ (250 mL) was prepared. At 0 °C, a solution of $PPh_3$ (3.67 g, 13.99 mmol) in $CH_2Cl_2$ (30 mL) was added. It was stirred for 1 h at 40 °C and for 3 days at room temperature. The resulting brown solution was filtered through Celite, and the filtrate was evaporated in vacuo. The brown solid was washed several times with hexane (total 100 mL) and recrystallized from $CH_2Cl_2$/hexane. A first fraction afforded traces of the *cis* product (IR ($cm^{-1}$): 1981 (s), 1889 (s)) as yellow-orange crystals. Adding more hexane afforded **2d** (5.06 g, 5.43 mmol, 81%) as a yellow powder. Analytically pure material is obtained after recrystallization from $Et_2O$. After drying for several days in vacuo, 0.7 equiv of $Et_2O$ could still be detected in the NMR spectrum. IR (KBr, $cm^{-1}$): 2024 (w), 1945 (s). $^1H$ NMR (300 MHz, $C_6D_6$, ppm): 7.91−7.88 (m, 12H, Ph), 6.97−6.89 (m, 18H, Ph), 6.32 (s, 2H, Mes), 2.00 (s, 3H, C*H*$_3$-Mes), 1.87 (s, 6H, 2C*H*$_3$-Mes). $^{13}C\{^1H\}$ NMR (75.4 MHz, $CD_2Cl_2$, ppm): 277.3 (t, $^2J_{CP}$ = 9.8 Hz, *C*Mes), 213.4 (t, $^2J_{CP}$ = 6.6 Hz, CO), 144.2 (t, $^3J_{CP}$ = 1.6 Hz, ipso-Mes), 139.4 (t, $^4J_{CP}$ = 6.6 Hz, *o*-Mes), 136.4 (s, *p*-Mes), 136.3 ("t", ipso-Ph), 134.2 ("t", *m*-Ph), 129.9 (s, *p*-Ph), 128.2 ("t", *o*-Ph), 127.9 (s, *m*-Mes), 21.4 (s, *C*H$_3$-Mes), 20.9 (s, 2*C*H$_3$-Mes). $^{31}P\{^1H\}$ NMR (121.5 MHz, $C_6D_6$, ppm): 22.5 (s, $^1J_{PW}$ = 275 Hz). MS (FAB-Neg, LM = $CH_2Cl_2$, M = NBOH, *m*/*z*, %): 875 ($M^+$ − 2 CO, 20), 870 ($M^+$ − $C_5H_5$, 100), 868 ($M^+$ − CO − Cl, 40), 840 ($M^+$ − 2 CO − Cl, 4), 641 ($M^+$ − CO − $PPh_3$, 15), 612 ($M^+$ − 2 CO − $PPh_3$, 95). Anal. Calcd for $C_{48}H_{41}ClO_2P_2W{\cdot}0.7(CH_3CH_2)_2O$ (931.11): C, 61.86; H, 4.89. Found: C, 61.81; H, 5.05.

***trans*-W(CMes)Cl(CO)$_2$(dppe) (2e).** dppe (1.48 g, 3.70 mmol, 1.05 equiv) was added to a solution of **1** (2.0 g, 3.54 mmol) in $CH_2Cl_2$ (100 mL), and the reaction mixture was stirred for 3 h at room temperature. A change in color from orange to yellow was observed. Evaporation in vacuo, washing with hexane (2 × 10 mL), and recrystallization from $CH_2Cl_2$/hexane afforded **2e** (2.64 g, 3.27 mmol, 92%) as a yellow powder. IR (KBr, $cm^{-1}$): 1997 (s), 1913 (s). $^1H$ NMR (200 MHz, $CDCl_3$, ppm): 7.82−7.76 (m, 4H, Ph), 7.74−7.70 (m, 4H, Ph), 7.42−7.26 (m, 8H, Ph), 7.24−7.18 (m, 4H, Ph), 6.51 (s, 2H, Mes), 3.15−2.85 (m, 2H, $PCH_2$), 2.70−2.40 (m, 2H, $PCH_2$), 2.11 (s, 6H, C*H*$_3$-Mes), 1.79 (s, 3H, C*H*$_3$-Mes). $^{13}C\{^1H\}$ NMR (50.3 MHz, $CDCl_3$, ppm): 271.4 (t, $^2J_{CP}$ = 9.2 Hz, *C*Mes), 215.0 (dd, $^2J_{CP}$ = 43.3 × 7.0 Hz, CO), 145.8 (s, ipso-Mes), 140.7 (s, *o*-Mes), 137.5 (s, *p*-Mes), 127.8 (s, *m*-Mes), 143.5, 140.5, 135.1, 134.4, 133.2, 133.0, 132.2, 130.4, 129.7, 128.6, 128.4, 128.2 ($C_6H_5$), 26.0 (dd, $^1J_{CP}$ = 26.4 Hz, $^2J_{CP}$ = 12.3 Hz, $PCH_2$), 21.3 (s, *C*H$_3$-Mes), 20.0 (s, 2*C*H$_3$-Mes). $^{31}P\{^1H\}$ NMR (121.5 MHz, $CDCl_3$, ppm): 40.3 (s, $^1J_{PW}$ = 229 Hz). MS (FAB-Neg, LM = $CH_2Cl_2$, M = NBOH, *m*/*z*, %): 805 ($M^+$, 2), 771 ($M^+$ − Cl, 20), 748 ($M^+$ − 2 CO, 100). Anal. Calcd for $C_{38}H_{35}O_2P_2ClW$ (804.94): C, 56.70; H, 4.38. Found: C, 56.13; H, 4.40.

***trans*-W(CMes)Cl(CO)(P(OMe)$_3$)$_3$ (3a).** A solution of **1** (3.0 g, 5.3 mmol) and $P(OMe)_3$ (6.2 mL, 53 mmol) in THF (180 mL) was refluxed for 16 h. The yellow-green solution was cooled and filtered through Celite, and the clear, red filtrate was evaporated in vacuo. After washing with hexane, and recrystallization from $Et_2O$ at −80 °C, **3a** (3.80 g, 5.1 mmol, 95%) was obtained as a yellow powder. IR (KBr, $cm^{-1}$): 1946 (s). $^1H$ NMR (200 MHz, $C_6D_6$, ppm): 6.67 (s, 2H, Mes), 3.64−3.57 (m, 27H, P(OMe)$_3$), 2.81 (s, 6H, C*H*$_3$-Mes), 2.01 (s, 3H, C*H*$_3$-Mes). $^{13}C\{^1H\}$ NMR (50.3 MHz, $CD_2Cl_2$, ppm): 262.0 (q, $^2J_{CP}$ = 15.7 Hz, CMes), 221.2 (dt, $^2J_{CP}$ = 63.7 × 10.4 Hz, CO), 145.8 (s, ipso-Mes), 140.7 (s br, *o*-Mes), 136.3 (s, *p*-Mes), 128.2 (s, *m*-Mes), 52.7, 52.5, 52.2 (s, P(OMe)$_3$), 21.3 (s, *C*H$_3$-Mes), 20.8 (s, 2*C*H$_3$-Mes). $^{31}P\{^1H\}$ NMR (121.5 MHz, $C_6D_6$, ppm): 148.7 (d, 2P, $^2J_{PP}$ = 39.5 Hz, $^1J_{PW}$ = 425 Hz), 143.5 (t, 1P, $^2J_{PP}$ = 39.5 Hz, $^1J_{PW}$ = 366 Hz). MS (FAB-Neg, LM = $CH_2Cl_2$, M = NBOH, *m*/*z*, %): 750 ($M^+$, 1), 715 ($M^+$ − Cl, 17), 625 ($M^+$ − P(OMe)$_3$, 10), 598 ($M^+$ − CO − P(OMe)$_3$, 25), 566 ($M^+$ − 2 CO − P(OMe)$_3$, 5). Anal. Calcd for $C_{20}H_{38}ClO_{10}P_3W$ (750.74): C, 32.00; H, 5.10. Found: C, 31.95; H, 4.54.

***trans*-W(CMes)Cl(CO)(PMe$_3$)$_3$ (3b). 2b** (120 mg, 0.21 mmol) was stirred in $PMe_3$ (2.5 mL) for 5 days at room temperature. After 3 days, the initial suspension has turned into a clear, orange solution. Evaporation in vacuo and recrystallization from $Et_2O$ afforded **3b** (115 mg, 0.19 mmol, 88%) as an orange powder. IR (KBr, $cm^{-1}$): 1891 (s). $^1H$ NMR (300 MHz, $C_6D_6$, ppm): 6.67 (s, 2H, Mes), 2.58 (s, 6H, C*H*$_3$-Mes), 2.03 (s, 3H, C*H*$_3$-Mes), 1.44 (m, 18H, $PMe_3$), 1.28 (m, 9H, $PMe_3$). $^{13}C\{^1H\}$ NMR (50.3 MHz, $d_8$-THF, ppm): 261.9 (q, $^2J_{CP}$ = 10.2 Hz, CMes), 233.1 (dt, $^2J_{CP}$ = 43.4 × 7.0 Hz, CO), 147.5 (s, br, ipso-Mes), 137.9 (s br, *o*-Mes), 134.0 ("q" br, *p*-Mes), 127.2 ("q" br, *m*-Mes), 23.9 (s, *C*H$_3$-Mes), 22.5 (m, $PMe_3$), 21.4 (s, 2*C*H$_3$-Mes), 20.1 (m, $PMe_3$). $^{31}P\{^1H\}$ NMR (121.5 MHz, $C_6D_6$, ppm): −25.4 (d, 2P, $^2J_{PP}$ = 19.8 Hz, $^1J_{PW}$ = 272 Hz), −30.8 (t, 1P, $^2J_{PP}$ = 19.8 Hz, $^1J_{PW}$ = 213 Hz). MS (FAB-Neg, LM = $CH_2Cl_2$, M = NBOH, *m*/*z*, %): 607 ($M^+$, 1), 530 ($M^+$ − $PMe_3$, 48), 502 ($M^+$ − CO − PMe, 100). Anal. Calcd for $C_{20}H_{38}ClOP_3W$ (606.74): C, 39.59; H, 6.31. Found: C, 39.71; H, 6.14.

***trans*-W(CMes)Cl(CO)({Ph$_2$PCH$_2$CH$_2$}$_2$PPh) (3d).** A solution of **3a** (1.50 g, 2.00 mmol) and $(Ph_2PCH_2CH_2)_2PPh$ (1.12 g, 2.1 mmol) in toluene (50 mL) was refluxed for 6 h. The orange-green solution was cooled and filtered through Celite, and the clear, orange filtrate was evaporated in vacuo. After washing with hexane, and recrystallization from toluene/hexane, **3d** (1.59 g, 1.74 mmol, 87%) was obtained as an orange powder. IR (KBr, $cm^{-1}$): 1882 (s). $^1H$ NMR (300 MHz, $C_6D_6$, ppm): 7.95−7.72 (m, 10H, Ph), 7.18−6.82 (m, 15H, Ph), 6.57 (s, 2H, Mes), 3.55−3.20 (m, 4H, $PCH_2$), 2.25−1.85 (m, 4H, $PCH_2$), 2.10 (s, 3H, C*H*$_3$-Mes), 2.02 (s, 6H, C*H*$_3$-Mes). $^{13}C\{^1H\}$ NMR (53.7 MHz, $CD_2Cl_2$, ppm): 268.9 (m, *C*Mes), 235.0 (m, CO), 147.2 (s, ipso-Mes), 145.6 (s, *o*-Mes), 135.4 (s, *p*-Mes), 125.6 (s, *m*-Mes), 134.1−127.9 (Ph), 33.6 (m, $(Ph_2PCH_2CH_2)_2$-PPh), 26.0 (m, $(Ph_2PCH_2CH_2)_2PPh$), 21.5 (s, *C*H$_3$-Mes), 20.8 (s, 2*C*H$_3$-Mes). $^{31}P\{^1H\}$ NMR (121.5 MHz, $C_6D_6$, ppm): 81.8 (t, 1P, $^2J_{PP}$ = 8.5 Hz, $^1J_{PW}$ = 202 Hz), 47.0 (d, 2P, $^2J_{PP}$ = 8.5 Hz, $^1J_{PW}$ = 294 Hz). MS (FAB-Neg, LM = THF, M = NBOH, *m*/*z*, %): 913 ($M^+$, 1), 884 ($M^+$ − CO, 30). Anal. Calcd for $C_{45}H_{44}ClOP_3W$ (913.07): C, 59.19; H, 4.86. Found: C, 58.73; H, 5.26.

***trans*-W(CMes)Cl(P(OMe)$_3$)$_4$ (4a). 3a** (200 mg, 0.27 mmol) was dissolved in $P(OMe)_3$ (10 mL), and the resulting mixture was transferred into a steel autoclave and then heated to 120 °C for 3 days. The solvent was then removed in vacuo and the residue washed with hexane to afford complex **4a** (178 mg, 0.21 mmol, 77%) as a brown powder. This compound seems to be unstable and decomposes after 1 h at room temperature (visible by $^{31}P$ NMR). A satisfactory elemental analysis of **4a** could not be obtained. $^1H$ NMR (300 MHz, $C_6D_6$, ppm): 6.70 (s, 2H, Mes), 3.75−3.52 (m, 36H, (P(OMe)$_3$)$_3$), 2.65 (s, 6H, 2C*H*$_3$-Mes), 1.98 (s, 3H, C*H*$_3$-Mes). $^{13}C\{^1H\}$ NMR (50.3 MHz, $C_6D_6$, ppm): 266 (m, CMes), 148.71 (s, *ipso*-Mes), 140.80 (s, *o*-Mes), 135.56 (s, *p*-Mes), 128.25 (s, *m*-Mes), 51.01 (d, $^2J_{CP}$ = 6.11 Hz, (P(OMe)$_3$)$_4$), 21.30 (s, 2CH$_3$-Mes), 20.70 (s, CH$_3$-Mes).

$^{31}P\{^1H\}$ NMR (121.5 MHz, $C_6D_6$, ppm): 148.60 (s, $^1J_{PW} = 430$ Hz).

**W(CMes)(CO)($\eta^2$-$H_2BH_2$)($P(OMe)_3$)$_2$ (5a).** $NaBH_4$ (71.8 mg, 0.90 mmol) was added to a solution of **3a** (0.46 g, 0.61 mmol) in THF (20 mL). It was stirred for 2 h at room temperature. A change in color from yellow to red was observed. Evaporation in vacuo yielded a dark red solid, which was suspended in hexane (30 mL) and filtered through Celite. The clear, red solution was concentrated in vacuo until a few millieters of solvent was left. Keeping the solution at −80 °C overnight afforded a red, crystalline product. The solution was decanted at low temperature. The crystals, which melt at room temperature, were dried in vacuo, leaving **5a** (0.31 g, 0.51 mmol, 83%) as a red oil. IR (hexane, $cm^{-1}$): 2458 (w, $BH_t$), 2417 (m, $BH_t$), 1925 (s). $^1H$ NMR (300 MHz, $d_8$-toluene, ppm): 6.49 (s, 2H, Mes), 3.39 (m, 18H, $P(OMe)_3$), 2.53 (s, 6H, C$H_3$-Mes), 1.89 (s, 3H, C$H_3$-Mes). $^1H\{^{11}B\}$ NMR (300 MHz, $d_8$-toluene, ppm): −2.0 (s, br, 1H, WHB), −4.1 (s, br, 1H, WHB). $^{13}C\{^1H\}$ NMR (75.4 MHz, $C_6D_6$, ppm): 294.5 (t, $^2J_{CP} = 15.0$ Hz, *C*Mes), 235.4 (t, $^2J_{CP} = 8.0$ Hz, CO), 146.4 (s br, ipso-Mes), 138.7 (s br, *o*-Mes), 137.4 (s, *p*-Mes), 128.5 (s, *m*-Mes), 52.0 (s, $P(OMe)_3$), 21.4 (s, *C*$H_3$-Mes), 21.0 (s, 2*C*$H_3$-Mes). $^{31}P\{^1H\}$ NMR (121.5 MHz, $d_8$-toluene, ppm): 165.2 (s, $^1J_{PW} = 430$ Hz). A satisfactory elemental analysis could not be obtained.

**W(CMes)($\eta^2$-$H_2BH_2$)(CO)($PMe_3$)$_2$ (5b).** According to the procedure described for **5a**, $NaBH_4$ (96 mg, 2.60 mmol) was reacted with **3b** (470 mg (0.84 mmol), yielding after workup **5b** (356 mg (0.70 mmol, 83%) as a red, hygroscopic powder. A satisfactory elemental analysis of **5b** could not be obtained. IR ($C_6H_6$, $cm^{-1}$): 2420 (w, $BH_t$), 2392 (m, $BH_t$), 1878 (s). $^1H$ NMR (300 MHz, $d_8$-THF, ppm): 6.67 (s, 2H, Mes), 2.31 (s, 6H, C$H_3$-Mes), 2.11 (s, 3H, C$H_3$-Mes), 1.56 (m, 18H, $PMe_3$). $^{13}C\{^1H\}$ NMR (75.4 MHz, $d_8$-THF, ppm): 294.1 (t, $^2J_{CP} = 10.6$ Hz, *C*Mes), 248.3 (t, $^2J_{CP} = 4.3$ Hz, CO), 147.2 (s, ipso-Mes), 136.3 (s, *o*-Mes), 135.6 (s, *p*-Mes), 128.7 (s, *m*-Mes), 21.5 (s, 2*C*$H_3$-Mes), 21.4 (s, *C*$H_3$-Mes), 20.3 ("t", $J_{CP} = 14.2$ Hz, $PMe_3$). $^{31}P\{^1H\}$ NMR (121.5 MHz, $C_6D_6$, ppm): −4.0 (s, $^1J_{PW} = 275$ Hz).

**W(CMes)($\eta^2$-$H_2BH_2$)(CO)($P(O^iPr)_3$)$_2$ (5c).** From the reaction of **2c** (822 mg, 0.94 mmol) with $NaBH_4$ (105 mg, 2.83 mmol), according to the procedure described for **5a**, **5c** (619 mg, 0.80 mmol) could be isolated as a red oil. A satisfactory elemental analysis of **5c** could not be obtained. IR (hexane, $cm^{-1}$): 2450 (w, $BH_t$), 2408 (m, $BH_t$), 1913 (s). $^1H$ NMR (300 MHz, $C_6D_6$, ppm): 6.61 (s, 2H, Mes), 4.92 (m, 6H, POC$H$($CH_3$)$_2$), 2.71 (s, 6H, C$H_3$-Mes), 1.95 (s, 3H, C$H_3$-Mes), 1.22 (m, 36H, POCH(C$H_3$)$_2$). $^{13}C\{^1H\}$ NMR (75.4 MHz, $C_6D_6$, ppm): 295.4 (t, $^2J_{CP} = 14.1$ Hz, *C*Mes), 238.2 (t, $^2J_{CP} = 8.0$ Hz, CO), 146.5 (s, ipso-Mes), 138.4 (s, *o*-Mes), 136.7 (s, *p*-Mes), 128.5 (s, *m*-Mes), 69.4 (s, POC$H$($CH_3$)$_2$), 23.9 (s, POCH(*C*$H_3$)$_2$), 21.5 (s, *C*$H_3$-Mes), 21.3 (s, 2*C*$H_3$-Mes). $^{31}P\{^1H\}$ NMR (121.5 MHz, $C_6D_6$, ppm): 159.8 (s, $^1J_{PW} = 426$ Hz).

**W(CMes)($\eta^2$-$H_2BH_2$)(CO)($PPh_3$)$_2$ (5d).** As described for **5a**, **2c** (478 mg, 0.51 mmol) was reacted with $NaBH_4$ (58.5 mg, 1.58 mmol) for 4 h. **5d** (384 mg, 0.43 mmol, 85%) is obtained as a red solid. IR ($C_6H$, $cm^{-1}$): 2442 (w, $BH_t$), 2401 (m, $BH_t$), 1893 (s). H NMR (300 MHz, $C_6D_6$, ppm): 7.84 (m, 12H, Ph), 7.65−7.58 (m, 6H, Ph), 7.05−6.90 (m, 27H, Ph), 6.47 (s, 2H, Mes), 2.11 (s, 6H, C$H_3$-Mes), 1.94 (s, 3H, C$H_3$-Mes). $^{13}C\{^1H\}$ NMR (75.4 MHz, $C_6D_6$, ppm): 299.1 (t, $^2J_{CP} = 10.5$ Hz, *C*Mes), 243.2 (t, $^2J_{CP} = 4.6$ Hz, CO), 147.0 (s, ipso-Mes), 138.1 (s, *o*-Mes), 137.2 (s, *p*-Mes), 128.6 (s, *m*-Mes), 137.7, 135.2, 135.1, 135.0, 134.1, 134.0, 132.0, 130.2, 129.6, 129.4, 128.8, 128.7 (s, Ph), 21.5 (s, *C*$H_3$-Mes), 20.9 (s, 2*C*$H_3$-Mes). $^{31}P\{^1H\}$ NMR (121.5 MHz, $C_6D_6$, ppm): 45.2 (s, $^1J_{PW} = 282$ Hz). MS (FAB-Neg, LM = $CH_2Cl_2$, M = NBOH, *m*/*z*, %): 886 ($M^+$, 30), 865 ($M^+ - CO$, 38). A satisfactory elemental analysis could not be obtained.

**W(CMes)($\eta^2$-$H_2BH_2$)($P(OMe)_3$)$_3$ (6a). 4a** (120 mg, 0.14 mmol) was reacted with $NaBH_4$ (16 mg, 0.42 mmol) in THF (5 mL) at room temperature for 4 h. Workup of the reaction mixture as described for **5a** resulted in a red-brown solid, which was dried in vacuo, leaving **6a** (79 mg, 0.11 mmol, 79%) as an oil. IR (hexane, $cm^{-1}$): 2447 (m, $BH_t$), 2413 (s, $BH_t$), 1839 (s, $BH_b$). $^1H$ NMR (300 MHz, $C_6D_6$, ppm): 6.72 (s, 2H, Mes), 3.63−3.44 (m, 27H, $P(OMe)_3$), 2.72 (s, 6H, $CH_3$-Mes), 1.99 (s, 3H, $CH_3$-Mes), −3.5 (br, WHB). $^{13}C\{^1H\}$ NMR (75.4 MHz, $d_8$-THF, ppm): 284.5 (q, $^2J_{CP} = 16.8$ Hz, *C*Mes), 148.4 (s, ipso-Mes), 138.9 (s, *o*-Mes), 135.7 (s, *p*-Mes), 128.6 (s, *m*-Mes), 52.3 (d, $P(OMe)_3$), 52.1 (s, $P(OMe)_3$), 21.6 (s, 2*C*$H_3$-Mes), 21.4 (s, 2*C*$H_3$-Mes). $^{31}P\{^1H\}$ NMR (121.5 MHz, $C_6D_6$, ppm): 184.7 (t, $^2J_{PP} = 19.7$ Hz, $^1J_{PW} = 615$ Hz), 167.0 (d, $^2J_{PP} = 19.7$ Hz, $^1J_{PW} = 434$ Hz). Anal. Calcd for $C_{19}H_{42}BP_3O_9W$ (702.12): C, 32.50; H, 6.03. Found: C, 33.28; H, 5.48.

***trans*-W(CMes)(CO)H($P(OMe)_3$)$_3$ (7a).** A solution of **5a** (250 mg, 0.41 mmol), $P(OMe)_3$ (49 $\mu$L, 0.42 mmol), and quinuclidine (46 mg, 0.41 mmol) in THF (20 mL) was stirred for 2 h at −20 °C. The solution turned from red to orange. Warming to room temperature led to decomposition of the product. **7a** was spectroscopically characterized in the reaction mixture. In NMR experiments, an NMR tube was charged with **5a**, $P(OMe)_3$ (1 equiv), quinuclidine (1 equiv), and $d_8$-THF (0.5 mL). The tube was stored at −20 °C, and after 2 h, **7a** could be detected in a yield of 80%, as determined by $^{31}P\{^1H\}$ NMR spectroscopy. IR (THF, −30 °C, $cm^{-1}$): 1935 (s). $^1H$ NMR (300 MHz, $d_8$-THF, −20 °C, ppm): 6.41 (s, 2P, Mes), 3.34−3.27 (m, 27H, $P(OMe)_3$), 2.25 (s, 6H, C$H_3$-Mes), 1.86 (s, 3H, C$H_3$-Mes), −4.66 (q, 1H, $^2J_{HP} = 33.6$ Hz, $^1J_{HW} = 24.1$ Hz). $^{13}C\{^1H\}$ NMR (75.4 MHz, $d_8$-THF, −20 °C, ppm): 273.5 (q, $^2J_{CP} = 12.1$ Hz, *C*Mes), 224.8 (dt, $^2J_{CP} = 37.7 \times 10.8$ Hz, CO), 148.0 (s, ipso-Mes), 139.6 (s br, *o*-Mes), 135.4 (s, *p*-Mes), 128.7 (s, *m*-Mes), 52.1, 51.8, 51.7, 51.4 ($P(OMe)_3$), 21.6 (s, *C*$H_3$-Mes), 21.5 (s, 2*C*$H_3$-Mes). $^{31}P\{^1H\}$ NMR (121.5 MHz, $d_8$-THF, −20 °C, ppm): 168.0 (d, 2P, $^2J_{PP} = 39.4$ Hz, $^1J_{PW} = 423$ Hz), 160.2 (t, 1P, $^2J_{PP} = 39.4$ Hz, $^1J_{PW} = 377$ Hz).

***trans*-W(CMes)(CO)H($PMe_3$)$_3$ (7b).** An NMR tube was charged with **5b** (40 mg, 0.08 mol), $PMe_3$ (8 $\mu$L, 0.08 mol), quinuclidine (9 mg, 0.08 mol), and $d_8$-THF. The solution immediately turned orange. After 48 h at 0 °C, **7b** was obtained in 40% yield, determined by $^{31}P\{^1H\}$ NMR spectroscopy. **7b** is not stable at room temperature and was spectroscopically characterized in the reaction mixture. $^1H$ NMR (300 MHz, $d_8$-THF, 0 °C, ppm): 6.59 (s, 2H, Mes), 2.42 (s, 6H, C$H_3$-Mes), 2.08 (s, 3H, C$H_3$-Mes), 1.62−1.50 (m, 27H, $PMe_3$), −2.65 (dt, $^2J_{HP} = 32.2 \times 24.4$ Hz, $^1J_{HW} = 25$ Hz, WH). $^{31}P$ NMR (121.5 MHz, $d_8$-THF, 0 °C, ppm): −28.7 (d, 2P, $^2J_{PP} = 23.6$ Hz, $^1J_{PW} = 264$ Hz), −32.3 (t, 1P, $^2J_{PP} = 23.6$ Hz, $^1J_{PW} = 224$ Hz).

***trans*-W(CMes)(CO)H({$Ph_2PCH_2CH_2$}$_2$PPh) (7d).** An NMR tube was charged with **5d** (41 mg, 0.046 mmol), ($Ph_2PCH_2CH_2$)$_2$PPh (24.8 mg, 0.046 mmol), quinuclidine (5.16 mg, 0.046 mmol), and $d_8$-THF (0.5 mL) and kept at −20 °C for 2 h. The solution turned orange, and **7d** could be detected in 70% yield, determined by $^{31}P\{^1H\}$ NMR spectroscopy. Warming to room temperature led to decomposition of **7d**, which was spectroscopically characterized in the reaction mixture. $^1H$ NMR (300 MHz, $d_8$-THF, −20 °C, ppm): 6.58 (s, 2H, Mes), 2.20−1.08 (m, br, $CH_2P$), 2.03 (s, 3H, $CH_3$-Mes), 1.84 (s, 6H, $CH_3$-Mes), −6.2 (q, $^2J_{HP} = 37.5$ Hz, WH). $^{13}C\{^1H\}$ NMR (53.7 MHz, $d_8$-THF, −50 °C, ppm): 206.3 (m, CO), 147.2 (s, ipso-Mes), 145.6 (s, *o*-Mes), 135.4 (s, *p*-Mes), 125.6 (s, *m*-Mes), 134.6−129.0 (Ph), 33.6 (m, PPh(*C*$H_2$)$_2$), 26.0 (m, $PPh_2CH_2$), 22.0 (s, $CH_3$-Mes), 21.4 (s, 2$CH_3$-Mes). $^{31}P\{^1H\}$ NMR (121.5 MHz, $d_8$-THF, −20 °C, ppm): 88.6 (t, 1P, $^2J_{PP} = 7.3$ Hz, $^1J_{PW} = 200$ Hz), 56.7 (d, 2P, $^2J_{PP} = 7.3$ Hz, $^1J_{PW} = 292$ Hz).

***trans*-W(CMes)H($P(OMe)_3$)$_4$ (8a).** In an NMR tube, **6a** (34 mg, 0.048 mmol) was dissolved in $d_8$-THF (0.8 mL). At −20 °C, quinuclidine (6.5 mg, 0.058 mmol) and $P(OMe)_3$ (10 $\mu$L, 0.059 mmol) were added. After the reaction mixture was kept at −20 °C overnight, **8a** could be detected in over 95% yield, determined by $^{31}P\{^1H\}$ NMR spectroscopy. At room temperature, **8a** decomposes within a few hours. It was therefore characterized by NMR spectroscopy of the reaction mixture. $^1H$ NMR (300 MHz, $d_8$-THF, ppm, −20 °C): 6.53 (s, 2H, Mes),

3.70−3.42 (m, 36H, $P(OMe)_3$), 2.49 (s, 6H, $CH_3$-Mes), 2.02 (s, 3H, $CH_3$-Mes), −5.58 (quint., $^2J_{HP}$ = 35.7 Hz, $^1J_{HW}$ = 20.4 Hz, WH). $^{13}C\{^1H\}$ NMR (75.4 MHz, $d_8$-THF, −20 °C, ppm): 265.0 (quint., $^2J_{CP}$ = 13.1 Hz, *C*Mes), 151.2 (quint., $^3J_{CP}$ = 1.8 Hz, ipso-Mes), 140.1 (quint., $^4J_{CP}$ = 2.0 Hz, *o*-Mes), 133.7 (s, *p*-Mes), 128.5 (s, *m*-Mes), 48.9 (d, $^2J_{CP}$ = 9.9 Hz, $P(OMe)_3$), 21.6 (s, 2*C*$H_3$-Mes), 21.5 (s, 2*C*$H_3$-Mes). $^{31}P\{^1H\}$ NMR (121.5 MHz, $d_8$-THF, ppm, −20 °C): 168.3 (s, $^1J_{PW}$ = 432 Hz).

***trans*-W(CMes)($\eta^1$-$HBH_3$)(CO)($P(OMe)_3$)$_3$ (9a).** An NMR tube is charged with **5a** (55 mg, 0.09 mmol) and $d_8$-THF (0.5 mL). At −60 °C, $P(OMe)_3$ (12 μL, 0.09 mmol) is added. The color immediately changes from red to orange. The yield was determined as 90% by $^{31}P\{^1H\}$ NMR spectroscopy. $^1H$ NMR (300 MHz, $d_8$-THF, −60 °C, ppm): 6.66 (s, 2H, Mes), 3.65−3.58 (m, 27H, $P(OMe)_3$), 2.51 (s, 6H, C$H_3$-Mes), 2.10 (s, 3H, C$H_3$-Mes), −1.95 (br, WHB). $^{31}P$ NMR (121.5 MHz, $d_8$-THF, −60 °C, ppm): 154.5 (d, 2P, $^2J_{PP}$ = 40.9 Hz, $^1J_{PW}$ = 425 Hz), 150.4 (t, 1P, $^2J_{PP}$ = 40.9 Hz, $^1J_{PW}$ = 362 Hz).

**W(CMes)($\eta^1$-$HBH_3$)(CO)($PMe_3$)$_3$ (9b). 5d** (54 mg, 0.061 mmol) and $PMe_3$ (25 μL, 0.243 mmol) are reacted in $d_8$-THF (0.5 mL) at −60 °C in an NMR tube. During the spectroscopic investigation, the temperature is kept below −20 °C. The spectroscopic yield amounts to 95%. $^1H$ NMR (300 MHz, $d_8$-THF, −30 °C, ppm): 6.65 (s, 2H, Mes), 2.45 (s, 6H, C$H_3$-Mes), 2.09 (s, 3H, C$H_3$-Mes), 1.67−1.63 (m, 27H, $PMe_3$), −2.1 (br, WHB). $^{13}C\{^1H\}$ NMR (75.4 MHz, $d_8$-THF, −20 °C, ppm): 274.8 (q, $^2J_{CP}$ = 10.2 Hz, *C*Mes), 233.7 (dt, $^2J_{CP}$ = 32.9 × 7.4 Hz, CO), 147.2 (s, ipso-Mes), 139.4 (s, *o*-Mes), 135.0 (s, *p*-Mes), 128.7 (s, *m*-Mes), 22.6 (s, 2*C*$H_3$-Mes), 22.1 (m, $PMe_3$), 21.4 (s, *C*$H_3$-Mes). $^{31}P$ NMR (121.5 MHz, $d_8$-THF, −30 °C, ppm): −24.9 (d, 2P, $^2J_{PP}$ = 20.1 Hz, $^1J_{PW}$ = 271 Hz), −30.1 (t, 1P, $^2J_{PP}$ = 20.1 Hz, $^1J_{PW}$ = 213 Hz).

**W(CMes)(CO)(OPh)($P(OMe)_3$)$_3$ (10).** A solution of **7a** (0.05 mmol) in $d_8$-THF (0.5 mL) was mixed with phenol (5 mg, 0.05 mmol) at −40 °C in an NMR tube. Within 24 h at 0 °C the formation of **10** and the evolution of $H_2$ was observed in the NMR spectra. The yield of product formation was 60%, determined by $^{31}P\{^1H\}$ NMR-spectroscopy. **10** was too unstable to be isolated from the reaction mixture. IR ($CH_2Cl_2$, $cm^{-1}$): 1958 (s). $^1H$ NMR (300 MHz, $d_8$-THF, 0 °C, ppm): 6.66 ("t", 2H, *m*-Ph), 6.38 (s, 2H, Mes), 6.27 ("d", 2P, *o*-Ph), 6.05 ("t", 1P, *p*-Ph), 3.55−3.42 (m, 27H, $P(OMe)_3$), 2.54 (s, 6H, C$H_3$-Mes), 2.20 (s, 3H, C$H_3$-Mes). $^{31}P$ NMR (121.5 MHz, $d_8$-THF, 0 °C, ppm): 150.3 (d, 2P, $^2J_{PP}$ = 39.4 Hz, $^1J_{PW}$ = 429 Hz), 142.0 (t, 1P, $^2J_{PP}$ = 39.4 Hz, $^1J_{PW}$ = 375 Hz).

**W(CMes)(CO)($\eta^1$-OC(O)H)($P(OMe)_3$)$_3$ (11).** To a solution of **5a** (200 mg, 0.33 mmol) in THF (30 mL) were added $P(OMe)_3$ (38.9 μL, 0.32 mmol) and quinuclidine (37 mg, 0.32 mmol) at −40 °C, After 2 h at −25 °C, the reaction vessel is flooded with $CO_2$ under vigorous stirring. Within a few minutes a color change from dark orange to orange was observed. After 30 min, the solution was slowly warmed to room temperature. After another 30 min, the solvent was evaporated in vacuo. The crude product was washed with hexane, suspended in $Et_2O$, and filtered through Celite. The filtrate was concentrated and kept at −80 °C. At this temperature, **11** (181 mg, 0.24 mmol, 72%) precipitated as an orange oil. IR ($CH_2Cl_2$, $cm^{-1}$): 1942 (s), 1623 (s). $^1H$ NMR (300 MHz, $d_8$-THF, ppm): 7.97 (q, $^4J_{HP}$ = 1.1 Hz, 1H, OC(O)H), 6.62 (s, 2H, Mes), 3.74−3.61 (m, 27H, $P(OMe)_3$), 2.57 (s, 6H, C$H_3$-Mes), 2.12 (s, 3H, C$H_3$-Mes). $^{13}C\{^1H\}$ NMR (75.4 MHz, $d_8$-THF, ppm): 271.0 (q, $^2J_{CP}$ = 14.8 Hz, CMes), 221.1 (dt, $^2J_{CP}$ = 64.3 × 10.9 Hz, CO), 167.1 (dt, $^3J_{CP}$ = 6.2 × 1.5 Hz, OC(O)H), 147.2 (s, ipso-Mes), 140.9 (s br, *o*-Mes), 136.1 (s, *p*-Mes), 128.5 (s, *m*-Mes), 54.2, 52.2, 52.0 (s, $P(OMe)_3$), 21.4 (s, *C*$H_3$-Mes), 21.1 (s, 2*C*$H_3$-Mes). $^{31}P\{^1H\}$ NMR (121.5 MHz, $d_8$-THF, ppm): 154.6 (d, 2P, $^2J_{PP}$ = 40.3 Hz, $^1J_{PW}$ = 430 Hz), 147.5 (t, 1P, $^2J_{PP}$ = 40.3 Hz, $^1J_{PW}$ = 380 Hz). MS (FAB-Neg, LM = THF, M = NBOH, *m*/*z*, %): 732 ($M^+$ − CO, 5), 715 ($M^+$ − COOH, 70), 608 ($M^+$ − $P(OMe)_3$ − CO, 12), 591 ($M^+$ − $P(OMe)_3$ − COOH, 14). A satisfactory elemental analysis could not be obtained.

**W(CMes){$\eta^2$-(*Z*)-C($CO_2$Me)=CH[C(O)OMe]}(CO)($P(OMe)_3$)$_2$ (12). 12** is prepared according to the procedure described for **11**. **7a** is generated in situ from **5a** (250 mg, 0.41 mmol), $P(OMe)_3$ (48.6 μL, 0.40 mmol), and quinuclidine (46 mg, 0.41 mmol) in THF (30 mL) and reacted with MeOOCC≡CCOOMe (51 μL, 0.42 mmol). **12** (265 mg, 0.36 mmol, 88%) was isolated as a red oil. IR ($CH_2Cl_2$, $cm^{-1}$): 1905 (s), 1699 (m), 1590 (m). $^1H$ NMR (300 MHz, $C_6D_6$, ppm): 6.91 (t, 2H, $^4J_{HP}$ = 3.5 Hz, H-vinyl), 6.69 (s, 2H, Mes), 3.51 ("t", 18H, $P(OMe)_3$), 3.60 (s, 3H, $OCH_3$), 3.24 (s, 3H, $OCH_3$), 2.84 (s, 6H, C$H_3$-Mes), 2.02 (s, 3H, C$H_3$-Mes). $^{13}C\{^1H\}$ NMR (53.7 MHz, $d_8$-THF, ppm): 280.9 (t, $^2J_{CP}$ = 15.6 Hz, CMes), 237.1 (t, $^2J_{CP}$ = 9.3 Hz, CO), 235.4 (t, $^2J_{CP}$ = 12.4 Hz, α-C(vinyl)), 183.6 (s, *C*OOMe), 179.5 (s, *C*OOMe), 147.6 (s, ipso-Mes), 140.0 (s br, *o*-Mes), 136.0 (s, *p*-Mes), 128.4 (s, *m*-Mes), 119.5 (t, $^3J_{CP}$ = 3.9 Hz, β-C(vinyl)), 54.2, 51.9 (s, $P(OMe)_3$), 21.5 (s, *C*$H_3$-Mes), 21.1 (s, 2*C*$H_3$-Mes). $^{31}P\{^1H\}$ NMR (121.5 MHz, $C_6D_6$, ppm): 160.7 (s, $^1J_{PW}$ = 433 Hz). MS (FAB-Neg, LM = THF, M = NBOH, *m*/*z*, %): 706 ($M^+$ − CO, 7), 610 ($M^+$ − $P(OMe)_3$, 7), 582 ($M^+$ − $P(OMe)_3$ − CO, 6). A satisfactory elemental analysis could not be obtained.

**W(CMes)(CO)($\eta^2$-$NC_5H_4${2-$CH_2O$})($P(OMe)_3$)$_2$ (13).** An NMR tube was charged with **5a** (21 mg, 34.6 mmol) and $d_8$-THF (0.5 mL). At −50 °C, $P(OMe)_3$ (4 μL, 33.9 mmol) and quinuclidine (3.8 mg, 34.2 mmol) were added, and the tube was kept for 2 h at −20 °C to form **7a**. Then, pyridine-2-carbaldehyde (4.7 μL, 49.2 mmol) was added. After 22 h the consumption of **7a** is complete. **13** is obtained in a yield of 80%, as determined by $^{31}P\{^1H\}$ NMR spectroscopy. Warming to room temperature leads to decomposition within 15 min. $^1H$ NMR (300 MHz, $d_8$-THF, −20 °C, ppm): 9.12 ("d", 1H, *J* = 5.6 Hz, H−C(6′)), 7.67 ("t", 1H, *J* = 7.5 Hz, H−C(4′)), 7.21 ("d", 1H, *J* = 7.9 Hz, H−C(3′)), 7.11 ("t", 1H, *J* = 6.4 Hz, H−C(5′)), 6.63 (s, 2H, Mes), 5.11 (t, 2H, $^4J_{HP}$ = 4.3 Hz, $CH_2O$), 3.52−3.41 (m, 18H, $P(OMe)_3$), 2.59 (s, 6H, $CH_3$-Mes), 2.13 (s, 3H, $CH_3$-Mes). $^{31}P$ NMR (121.5 MHz, $d_8$-THF, −20 °C, ppm): 148.8 (s, $^1J_{PW}$ = 437 Hz).

**W(CMes)(CO)($\eta^2$-$NC_5H_4${2-CH(Ph)O})($P(OMe)_3$)$_2$ (14).** As described for **13**, **7a** is reacted with 1.0 equiv of benzoylpyridine. After 48 h all of **7a** has reacted. **14** is detected in a yield of 25%, by $^{31}P\{^1H\}$ NMR spectroscopy. $^1H$ NMR (300 MHz, $d_8$-THF, −20 °C, ppm): 9.20 ("d", 1H, H−C(6′)), 8.05−7.95 (m, 2H, Ph), 7.62 ("t", 1H, H−C(4′)), 7.60−7.40 (m, 3H, Ph), 7.17 ("d", 1H, H−C(3′)), 7.13 ("t", 1H, H−C(5′)), 6.77 (s, 2H, Mes), 5.67 (t, 1H, $^4J_{HP}$ = 5.7 Hz, CHO), 3.63−3.45 (m, 18H, $P(OMe)_3$), 2.62 (s, 6H, C$H_3$-Mes), 2.28 (s, 3H, C$H_3$-Mes). $^{31}P$ NMR (121.5 MHz, $d_8$-THF, −20 °C, ppm): 149.7 (d, $^2J_{PP}$ = 183.3 Hz, $^1J_{PW}$ = 437 Hz).

**W(CHMes)(CO)($P(OMe)_3$)$_4$ (15a).** A solution of **7a** in $d_8$-THF (0.5 mL) is treated with a varying excess of $P(OMe)_3$ (1.0−3.0 equiv). At −30 °C and below, complex **15a** was detected to be in equilibrium with **7a** by IR and NMR spectroscopy. IR (THF, −30 °C, $cm^{-1}$): 1803 (s). $^1H$ NMR (300 MHz, $d_8$-THF, −50 °C, ppm): 16.92 (m br, C*H*Mes), 6.71 (s, 2P, Mes), 3.81−3.48 (m, 36H, $P(OMe)_3$), 2.62 (s, 3H, C$H_3$-Mes), 2.55 (s, 6H, C$H_3$-Mes). $^1H\{^{31}P_{selective}\}$ NMR (300 MHz, $d_8$-THF, −50 °C, ppm): 16.92 (ddt, $^3J_{HP}$ = 30.2 × 10.9 × 14.8 Hz, C*H*Mes). $^{13}C\{^1H\}$ NMR (75.4 MHz, $d_8$-THF, −45 °C, ppm): 287.7 (s br, C*H*Mes), 219.1 (ddt, $^2J_{CP}$ = 58.8 × 7.5 × 11.1 Hz, CO), 149.2 (s, ipso-Mes), 139.5 (s br, *o*-Mes), 129.4 (s, *m*-Mes). $^{31}P\{^1H\}$ NMR (121.5 MHz, $d_8$-THF, −50 °C, ppm): 165.3 (dt, 1P, $^2J_{PP}$ = 51.7 × 22.4 Hz, $^1J_{PW}$ = 235 Hz), 154.2 (dd, 2P, $^2J_{PP}$ = 51.7 × 36.4 Hz, $^1J_{PW}$ = 420 Hz), 130.0 (dt, 1P, $^2J_{PP}$ = 36.4 × 22.4 Hz, $^1J_{PW}$ = 328 Hz).

**W(CHMes)(CO)($PMe_3$)$_2$($P(OMe)_3$)$_2$ (15b).** A solution of **7a** (0.13 mmol) in $d_8$-THF (0.5 mL) is treated with $PMe_3$ (39 μL, 0.39 mmol) at −50 °C. The solution turned dark orange, and **15** was obtained in 80% yield, determined by $^{31}P\{^1H\}$ NMR spectroscopy. At 0 °C, decomposition took place within a few minutes. $^1H$ NMR (300 MHz, $d_8$-THF, −20 °C, ppm): 16.32 (m, 1H, C*H*Mes), 6.59 (s, 2P, Mes), 3.69−3.42 (m, 18H,

$P(OMe)_3$), 2.21 (s, 3H, C*H*$_3$-Mes), 2.08 (s, 6H, C*H*$_3$-Mes), 0.95 (m, 18H, $PMe_3$). $^{13}C\{^1H\}$ NMR (75.4 MHz, $d_8$-THF, −20 °C, ppm): 274.9 (m, *C*HMes), 223.3 (m, CO), 143.5 (s, ipso-Mes), 134.7 (s br, *o*-Mes), 131.9 (s, *p*-Mes), 131.3 (s, *m*-Mes), 51.4 ($P(OMe)_3$), 25.7 (m, $PMe_3$), 22.0 (s, 2*C*H$_3$-Mes), 21.5 (s, *C*H$_3$-Mes). $^{31}P\{^1H\}$ NMR (121.5 MHz, $d_8$-THF, −20 °C, ppm): 150.9 (dd, $2P(OMe)_3$, $^2J_{PP} = 41.8 \times 29.0$ Hz, $^1J_{PW} = 425$ Hz), −38.3 (td, $1PMe_3$, $^2J_{PP} = 29.0 \times 5.9$ Hz, $^1J_{PW} = 189$ Hz), −38.9 (td, $1PMe_3$, $^2J_{PP} = 41.8 \times 5.9$ Hz, $^1J_{PW} = 123$ Hz).

**W(CHMes)(CO)$_2$(P(OMe)$_3$)$_3$ (16).** An NMR tube, containing a solution of **7a** in $d_8$-THF, was flooded with CO gas at −50 °C. A color change from orange to yellowish black was observed, and **16** was obtained in a spectroscopic yield of 75%. Warming to 0 °C led to decomposition within a few minutes. IR (THF, −30 °C, cm$^{-1}$): 2001 (m), 1877 (s). $^1H$ NMR (300 MHz, $d_8$-THF, −30 °C, ppm): 16.36 (q, 1H, $^3J_{HP} = 4.3$ Hz, C*H*Mes), 6.67 (s, 2H, Mes), 3.66−3.39 (m, 27H, $P(OMe)_3$), 2.31 (s, 6H, C*H*$_3$-Mes), 2.10 (s, 3H, C*H*$_3$-Mes). $^{13}C$ NMR (75.4 MHz, $d_8$-THF, −30 °C, ppm): 283 (s, br, *C*HMes), 208 (s, br, CO). $^{31}P$ NMR (121.5 MHz, $d_8$-THF, −30 °C, ppm): 158.5 (t, 1P, $^2J_{PP} = 48.0$ Hz, $^1J_{PW} = 232$ Hz), 154.7 (d, 2P, $^2J_{PP} = 48.0$ Hz, $^1J_{PW} = 414$ Hz).

**W(CHMes)Cl$_2$(CO)(P(OMe)$_3$)$_2$ (17).** A solution of **3a** (262 mg, 0.35 mmol) in THF (50 mL) was cooled to −25 °C, and a 1.0 M solution of HCl in $Et_2O$ (0.4 mL, 0.40 mmol) was added. After 5 min, the reaction mixture was warmed to room temperature, and the dark orange solution was stirred for 1 h. The solvent was evaporated in vacuo, and the resulting brown oil was recrystallized from hexane. **17** (160 mg, 0.25 mmol, 70%) was isolated as a temperature-sensitive, red crystalline material. IR (KBr, cm$^{-1}$): 1960 (s). $^1H$ NMR (300 MHz, $C_6D_6$, ppm): 6.51 (s, 2H, Mes), 3.61 (m, 18H, $P(OMe)_3$), 2.67 (s, 6H, C*H*$_3$-Mes), 1.96 (s, 3H, C*H*$_3$-Mes), −0.38 (t, 1H, $^3J_{HP} = 4.8$ Hz, $^1J_{HW} = 28.7$ Hz, $^1J_{HC} = 75.2$ Hz, C*H*Mes). $^{13}C\{^1H\}$ NMR (53.7 MHz, $C_6D_6$, ppm): 228.0 (t, $^2J_{CP} = 8.6$ Hz, *C*HMes), 217.9 (t, $^2J_{CP} = 16.0$ Hz, CO), 52.9 (s, $P(OMe)_3$), 21.1 (s, 1C$H_3$-Mes), 20.8 (s, 2C$H_3$-Mes). $^{31}P\{^1H\}$ NMR (121.5 MHz, $C_6D_6$, ppm): 127.7 (s, $^1J_{PW} = 415$ Hz). MS (FAB-Neg, LM = $CH_2Cl_2$, M = NBOH, *m*/*z*, %): 664 ($M^+$, 1), 626 ($M^+ - Cl$, 15), 600 ($M^+ - CO - Cl$, 28), 567 ($M^+ - CO - 2\ Cl$, 10).

**Computational Procedures. General Considerations.** The density functional[28](DF) calculations utilized the ADF[29] program package, release 1999.01/02 and 2.0.1. For the *n*s, *n*p, *n*d, and (*n* + 1)s shells on W, a triple-ζ-STO basis augmented by one (*n* + 1)p function was employed (ADF database IV). The valence shell of main-group elements was described by a double-ζ-STO basis and one STO polarization function (ADF database III). The numerical integration grid was chosen in a way that significant test integrals are evaluated with an accuracy of at least four significant digits. The self-consistent DF calculations were based on the local exchange-correlation potential of Vosko, Wilk, and Nussair,[30] with self-consistent gradient corrections due to Becke[31] and Perdew[32] (BP86). Relativistic effects were included using a quasi-relativistic approach.[33]

**Geometry Optimization.** Default procedures[34] were applied in geometry optimizations and transition state (TS) searches. Final gradients were better than 0.003 hartree/Å or hartree/radian, respectively. The start geometries for the TS optimizations were obtained in a linear transit run along the respective internal mode. The TS were identified by one negative eigenvalue of the approximate Hessian.

**Chemical Model.** Modeling $POMe_3$ by $PH_3$ will influence the energetics of those reaction sequences, which involve dissociation or association of a phosphorus ligand, in the sense that the phosphite forms stronger M−L bonds.[35] Reactions in which the framework of the P ligands does not significantly change are less affected by this simplification. On the other hand, solvent effects can be expected to lower the free enthalpy for M−L bond dissociation. Thus, the model reactions studied in this work should provide an approximate but reasonable description of the hydride migration as well as carbene formation processes as observed in the experiment.

**Acknowledgment.** Financial support from the Swiss National Science Foundation (SNSF) is gratefully acknowledged.

**Supporting Information Available:** Figures giving selected $^1H$ NMR spectra for **15a**, **16**, and **17** and tables giving Cartesian coordinates and final bonding energies for the optimized geometries **I**−**XVIII**.

OM000129H

(28) (a) Kohn, W.; Becke, A. D.; Parr, R. G. *J. Phys. Chem.* **1996**, *100*, 12974. (b) Baerends, E. J.; Gritsenko, O. V. *J. Phys. Chem. A* **1997**, *101*, 5383.

(29) (a) Baerends, E. J.; Bérces, A.; Bo, C.; Boerrigter, P. M.; Cavallo, L.; Deng, L.; Dickson, R. M.; Ellis, D. E.; Fan, L.; Fischer, T. H.; Fonseca Guerra, C.; van Gisbergen, S. J. A.; Groeneveld, J. A.; Gritsenko, O. V.; Harris, F. E.; van den Hoek, P.; Jacobsen, H.; van Kessel, G.; Kootstra, F.; van Lenthe, E.; Osinga, V. P.; Philipsen, P. H. T.; Post, D.; Pye, C. C.; Ravenek, W.; Ros, P.; Schipper, P. R. T.; Schreckenbach, G.; Snijders, J. G.; Sola, M.; Swerhone, D.; te Velde, G.; Vernooijs, P.; Versluis, L.; Visser, O.; van Wezenbeek, E.; Wiesenekker, G.; Wolff, S. K.; Woo, T. K.; Ziegler, T. ADF Release 1999.02, SCM, Amsterdam, 1999. (b) Baerends, E. J.; Ellis, D. E.; Ros, P. E. *Chem. Phys.* **1973**, *2*, 41. (c) te Velde, G.; Baerends, E. J. *J. Comput. Phys.* **1992**, *99*, 84. (d) Fonseca Guerra, C.; Snijders, J. G.; te Velde, G.; Baerends, E. J. *Theor. Chem. Acta* **1998**, *99*, 391.

(30) Vosko, S. J.; Wilk, M.; Nussair, M. *Can. J. Phys.* **1980**, *58*, 1200.

(31) Becke, A. *Phys. Rev.* **1988**, *A38*, 3098.

(32) Perdew, J. P. *Phys. Rev.* **1986**, *B33*, 8822.

(33) Ziegler, T.; Tschinke, V.; Baerends, E. J.; Snijders, J. G.; Ravenek, W. *J. Phys. Chem.* **1989**, *93*, 3050.

(34) te Velde, G. *ADF User's Guide*, Vrije Universiteit Amsterdam: Amsterdam, 1999.

(35) Bannwart, E.; Jacobsen, H.; Hübener, R.; Schmalle, H. W.; Berke, H. Submitted for publication.